

# Visualizing classification results

Jakob Raymaekers, Peter J. Rousseeuw, and Mia Hubert

Section of Statistics and Data Science,  
Department of Mathematics, KU Leuven, Belgium

September 10, 2020

## Abstract

Classification is a major tool of statistics and machine learning. A classification method first processes a training set of objects with given classes (labels), with the goal of afterward assigning new objects to one of these classes. When running the resulting prediction method on the training data or on test data, it can happen that an object is predicted to lie in a class that differs from its given label. This is sometimes called label bias, and raises the question whether the object was mislabeled. Our goal is to visualize aspects of the data classification to obtain insight. The proposed display reflects to what extent each object's label is (dis)similar to its prediction, how far each object lies from the other objects in its class, and whether some objects lie far from all classes. The display is constructed for discriminant analysis, the k-nearest neighbor classifier, support vector machines, logistic regression, and majority voting. It is illustrated on several benchmark datasets containing images and texts.

*Keywords:* discriminant analysis, fairness, mislabeling, k-nearest neighbors classification, support vector machines.

## 1 Introduction

Classification is a major tool of statistics and machine learning. For an extensive introduction to classification methods see Hastie et al. (2017). A classification method first processes a training set of objects with given classes (labels), with the goal of afterward assigning new objects to one of these classes. When running the resulting prediction method on the training data or on validation data or test data, it can happen that an object is predicted to lie in a class that differs from its given label. This is sometimes called label

bias, and raises the question whether the object might have been mislabeled. Our goal is to visualize aspects of the data classification to obtain insight. For consistency, we will depict the predictions in the vertical direction throughout.

We start with a simple illustrative example. The flower bud data originate from Wouters et al. (2015) and were kindly provided to us by Dr. Bart De Ketelaere. They arose from an experiment in a pear orchard with the goal of detecting floral buds in their environment with branches, bud scales, and supports for the trees. The data contain 550 observations and 6 variables. There are four classes: branch (49 members), bud (363), bud scales (94 members), and support (44). We will represent them by colors reminiscent of each.

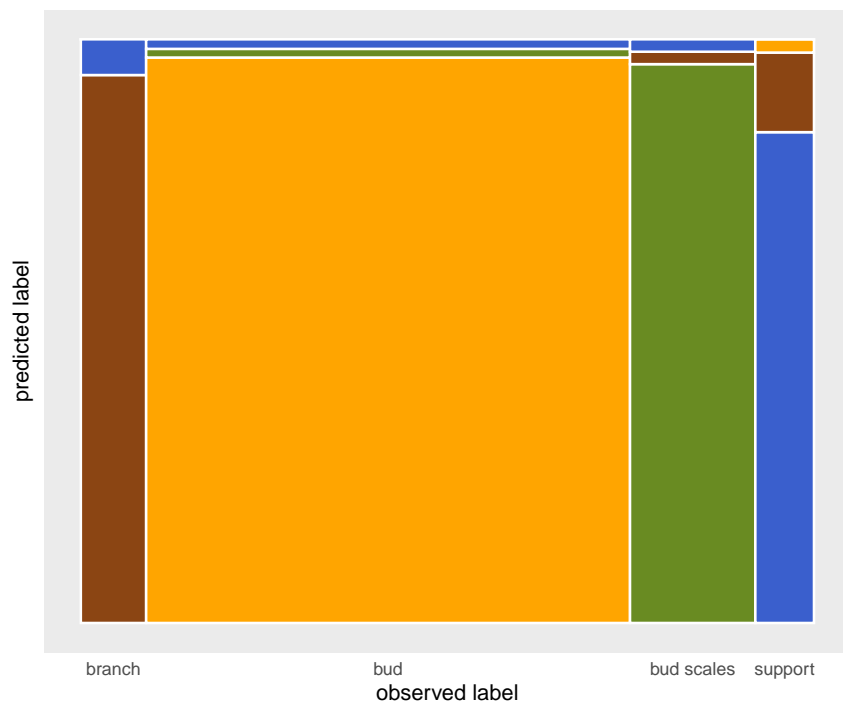


Figure 1: A stacked mosaic plot of a classification of the floral bud data. The given classes (labels) are on the horizontal axis, and the predicted labels are on the vertical axis. The area of each rectangle is proportional to the number of objects in it.

After a classification is carried out, we can display the result in a stacked bar chart or a mosaic plot (Hartigan and Kleiner, 1981; Friendly, 1994). Figure 1 shows such a stacked mosaic plot, which graphically represents the confusion matrix. The observed (given) classes are on the horizontal axis, and the predicted labels are on the vertical axis. The area of each rectangle is proportional to the number of objects in it. The display

immediately shows that the classes have different numbers of objects. Several variations of this plot are possible. One could rank the vertical labels in the order of the original classes, but we choose to put the given class at the bottom so that the lower part of each bar reflects the objects that were classified in accordance with their label. For the other labels in each bar we take the order of the remaining original classes. Here we see that buds are often classified correctly but that there is some confusion between branch and support.

Figure 1 does not yet give us an idea why some object is predicted to belong to a different class. Is it because the object lies in or near a region where classes overlap? Or is it deeply inside its predicted class and far from its given class, arousing suspicion that its original label was wrong? Or is it actually far from both its given and predicted classes? To assist with these questions we will propose a display that incorporates additional information.

Section 2 outlines the basic notions of label dissimilarity and farness, which can be computed for different data types. The subsequent sections apply these principles to several classification methods such as discriminant analysis, the k-nearest neighbor method, support vector machines, logistic regression, and majority voting.

## 2 Label dissimilarity and farness

Suppose we have objects denoted by their index  $i$  where  $i = 1, \dots, n$  and there are classes (groups, labels)  $g$  with  $g = 1, \dots, G$ . The target is thus a discrete variable with  $G$  levels. We wish to measure to what extent the given label  $g_i$  agrees with the classification. A classifier typically assigns the object  $i$  to the class  $g$  which attains the highest value of a criterion  $\varphi(i, g)$ . (If the assignment happens by minimizing a criterion, we just flip its sign.) We then define the highest criterion value attained by a label different from  $g_i$  as

$$\tilde{\varphi}(i) = \max\{\varphi(i, g); g \neq g_i\} . \quad (1)$$

This is the criterion value of the best competing label. If  $\varphi(i, g_i) > \tilde{\varphi}(i)$  it follows that  $g_i$  attains the overall highest value of  $\varphi(i, g)$  so the classifier agrees with the given label  $g_i$ . On the other hand, if  $\varphi(i, g_i) < \tilde{\varphi}(i)$  the classifier does not assign object  $i$  to label  $g_i$ . We quantify this by the *criterion difference*

$$\Delta(i) = \tilde{\varphi}(i) - \varphi(i, g_i) \quad (2)$$

which gives more information than its sign alone, since it reflects to what extent  $g_i$  outperforms or is outperformed by the competition, in the eyes of the classifier. Comparing with the best competitor to quantify how well an object is positioned inside its class was the main idea of the silhouette display for unsupervised classification (Rousseeuw, 1987). In fact,  $\Delta(i)$  of (2) is the numerator of the silhouette width when  $\varphi(i, g)$  is minus the average dissimilarity of object  $i$  to the objects in cluster  $g$ .

The  $\Delta(i)$  still needs to be normalized to become comparable across classes. In the definition of silhouettes the  $\Delta(i)$  were normalized such as to always lie between  $-1$  and  $1$ . Here we will normalize so the result always lies between  $0$  and  $1$ . The actual normalization depends on the classification criterion  $\varphi$  and is specified in the next sections. The normalized  $\Delta(i)$  will be called the *label dissimilarity*  $LD(i)$ , such that  $LD(i) \approx 0$  corresponds to a label that fits very well and  $LD(i) \approx 1$  to a label that does not fit well at all. The boundary between predicting the given label  $g_i$  or not will be at  $0.5$ .

The second component of the proposed display is a measure of *farness*  $f(i, g)$  of an object  $i$  from a class  $g$ , again in the eyes of the classifier. Unlike the  $\Delta(i)$  of (2), which is used for all classifiers in this paper, the definition of farness has to depend on the classifier because different classifiers make different assumptions about the data. For instance, discriminant analysis assumes roughly elliptical point clouds, k-nearest neighbors assume no particular shape but focus on local inter-point dissimilarities, and support vector machines allow for disconnected classes. We will specify the farness measures used as we go along.

We propose to draw a so-called *class map* for each class  $g$ , which plots the label dissimilarity  $LD(i)$  of all objects  $i$  in  $g$  versus their farness  $f(i, g)$ . Figure 2 is such a class map where  $g$  is the class of bud scales in Figure 1. The green points were predicted to lie in  $g$ , but a few points were predicted in a different class, corresponding to their color. We will describe the components of the class map one by one in the sequel.

Note that the proposed displays are intended to learn more about the objects in a given classification. They are not meant for comparing different types of classifiers on the same data set, for which other tools are available such as the misclassification rate.

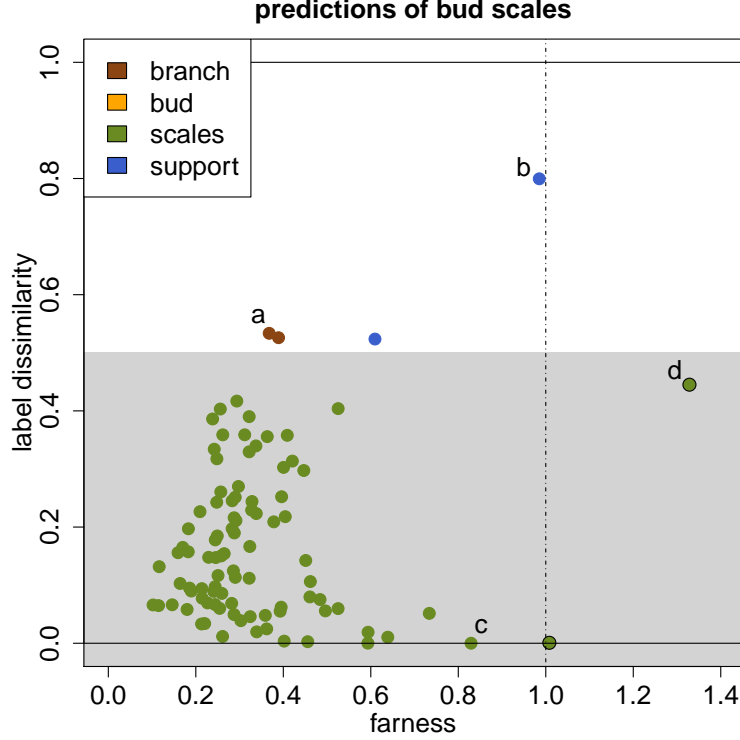


Figure 2: Example of a class map.

### 3 Discriminant analysis

One of the oldest and best understood classification techniques is discriminant analysis (DA), intended for objects that can be represented as points  $\mathbf{x}_i$  with  $d$  coordinates (measurements). The underlying model is the normal mixture model as described in e.g. Chapter 3 of McLachlan (2004). It assumes the points in class  $g$  follow a multinormal distribution  $N(\boldsymbol{\mu}_g, \boldsymbol{\Sigma}_g)$  with unknown class mean  $\boldsymbol{\mu}_g$  and covariance matrix  $\boldsymbol{\Sigma}_g$ , and unknown class probability  $p_g$ . In general all the  $\boldsymbol{\Sigma}_g$  are different. To train the classifier we compute estimates  $\hat{\boldsymbol{\mu}}_g$  and  $\hat{\boldsymbol{\Sigma}}_g$  which are typically the empirical mean and covariance of the points  $\mathbf{x}_i$  in class  $g$ . The class probability  $p_g$  is estimated as  $\hat{p}_g := n_g/n$  where  $n_g$  is the number of objects in class  $g$ . The estimated density of the mixture distribution is then  $\sum_g \hat{p}_g \phi(\mathbf{x}, \hat{\boldsymbol{\mu}}_g, \hat{\boldsymbol{\Sigma}}_g)$  with  $\phi$  the multinormal density. When a new data point  $\mathbf{x}$  arrives, Quadratic Discriminant Analysis (QDA) assigns it to the class  $g$  with highest  $\hat{p}_g \phi(\mathbf{x}, \hat{\boldsymbol{\mu}}_g, \hat{\boldsymbol{\Sigma}}_g)$ . Equivalently,  $\mathbf{x}$  is assigned to the class with highest log likelihood  $\ell(\mathbf{x}, g) := \log(\hat{p}_g \phi(\mathbf{x}, \hat{\boldsymbol{\mu}}_g, \hat{\boldsymbol{\Sigma}}_g))$  given by

$$\ell(\mathbf{x}, g) = \log(\hat{p}_g) - \frac{d}{2} \log(2\pi) - \frac{1}{2} \log(\det(\hat{\boldsymbol{\Sigma}}_g)) - \frac{1}{2} \text{MD}^2(\mathbf{x}, \hat{\boldsymbol{\mu}}_g, \hat{\boldsymbol{\Sigma}}_g) \quad (3)$$

where  $\text{MD}^2(\mathbf{x}, \hat{\boldsymbol{\mu}}_g, \hat{\boldsymbol{\Sigma}}_g) := (\mathbf{x} - \hat{\boldsymbol{\mu}}_g)' \hat{\boldsymbol{\Sigma}}_g^{-1} (\mathbf{x} - \hat{\boldsymbol{\mu}}_g)$  is the squared Mahalanobis distance. Dropping the constant term  $-\frac{d}{2} \log(2\pi)$  from (1) yields the so-called discriminant scores.

When we assume that all  $\boldsymbol{\Sigma}_g$  are equal we only need a single covariance estimate. We can for instance compute  $\hat{\boldsymbol{\Sigma}}$  from the pooled data  $\tilde{\mathbf{x}}_i := \mathbf{x}_i - \hat{\boldsymbol{\mu}}_{g_i}$  for  $i = 1, \dots, n$  where  $g_i$  is the label of object  $i$ . We then set all  $\hat{\boldsymbol{\Sigma}}_g := \hat{\boldsymbol{\Sigma}}$  and apply the same rule (3). This is called Linear Discriminant Analysis (LDA) because when comparing (3) for different  $g$  the quadratic terms cancel, leaving a linear criterion.

Both the QDA and LDA classifiers use the criterion  $\varphi(i, g) = \ell(\mathbf{x}_i, g)$ , so we can compute  $\tilde{\varphi}(i)$  and  $\Delta(i)$  from (1) and (2). Note that  $\Delta(i)$  can be any real number. In order to obtain a level dissimilarity in the interval  $[0, 1]$  we normalize it to

$$\text{LD}(i) = \text{logist}\left(\frac{\Delta(i)}{\text{median}_j |\Delta(j)|}\right) \quad (4)$$

where the sigmoid  $\text{logist}(z) = \exp(z)/(1 + \exp(z))$  is the logistic function. Note that  $\text{LD}(i)$  can be computed for any Bayes rule classifier using the same formulas, with the posterior density  $\sum_g \hat{p}_g f_g(\mathbf{x})$  and  $\varphi(i, g) = \log(\hat{p}_g f_g(\mathbf{x}_i))$ .

In Figure 2 the  $\text{LD}(i)$  are plotted on the vertical axis. The grey zone goes from 0 to 0.5. When  $\text{LD}(i) \leq 0.5$  (i.e.  $\Delta(i) \leq 0$ ) the given label  $g_i$  attains the highest value of (3), so the object is predicted in its given class (bud scales) and plotted in the green color of that class. On the other hand, when  $\text{LD}(i) > 0.5$  a different predicted label  $\hat{g}_i$  outperforms the given label. Here only few  $\text{LD}(i)$  exceed 0.5. Point **a** (in brown, hence predicted as branch) lies only slightly above it so it is a borderline case, but point **b** lands much higher. The graphical analogy is that of a fish out of water (the grey zone). When  $\text{LD}(i)$  is rather high one may want to check whether the original label was correct. Note that a high  $\text{LD}(i)$  does not imply certainty that the object  $i$  was mislabeled because there may be other causes, such as an error in  $\mathbf{x}_i$  or unsuitability of the chosen classifier for the data at hand.

On the other hand, a value of  $\text{LD}(i)$  much lower than 0.5, perhaps even close to 0, means that the given label  $g_i$  is especially appropriate since it not only coincides with the predicted label, but it also outperforms the second best label by a wide margin. Many points in the display, such as **c**, are in that situation.

The second ingredient of the class map is the farness. In the setting of discriminant

analysis it is natural to set the farness  $f(i, g)$  of object  $i$  to class  $g$  equal to

$$f(i, g) := \text{MD}(\mathbf{x}_i, \hat{\boldsymbol{\mu}}_g, \hat{\boldsymbol{\Sigma}}_g) \quad (5)$$

which is the Mahalanobis distance used in the classification criterion (3). The horizontal axis of Figure 2 shows the farness  $f(i, g)$  of each object  $i$  in the class  $g$  of bud scales. We see that point **d** is the furthest away from its given class, but as it is colored green it is still predicted to belong to this class.

The dashed vertical line is a rough cutoff suggesting that points to the right of it are unusually far, like point **d** in this map. The standard way to obtain a cutoff of the MD is to take a high (say, 99.5%) quantile of the  $\sqrt{\chi^2}$  distribution with degrees of freedom equal to the data dimension. However, this is not always accurate since the actual data distribution is often nonnormal. Therefore, we improve the initial cutoff by transforming the farness  $f(i, g_i)$  of all points  $i = 1, \dots, n$  with the aim of bringing the central part of the distribution close to univariate normal, using the technique of Raymaekers and Rousseeuw (2020). We then compute a standard cutoff on those data and transform back. Finally, all farness values are divided by that cutoff, so in each map the cutoff ends up at 1.

A final piece of information incorporated in the class map is whether a point with unusually large farness to its own class has an unexceptional farness to some other class. To find out we compute the ‘overall outlyingness’ of each object  $i$  as

$$O(i) = \min_{g=1, \dots, G} f(i, g) \quad (6)$$

and when  $O(i) > 1$  we put more emphasis on that point by using a different plotting symbol which has a black border around it. For such a point no class seems really suitable. In Figure 2 this happens for point **d** (and one other point with merely borderline farness). A point with high  $\text{LD}(i)$  but fairly low farness can instead be interpreted to lie in an overlapping region between classes.

Figure 3 visualizes the entire classification with all four classes together. Also in the class map of buds there are many objects with a low LD, that are well within their class. The class maps of branches and supports are more shallow, indicating that the classifier is less convinced about its assignments.

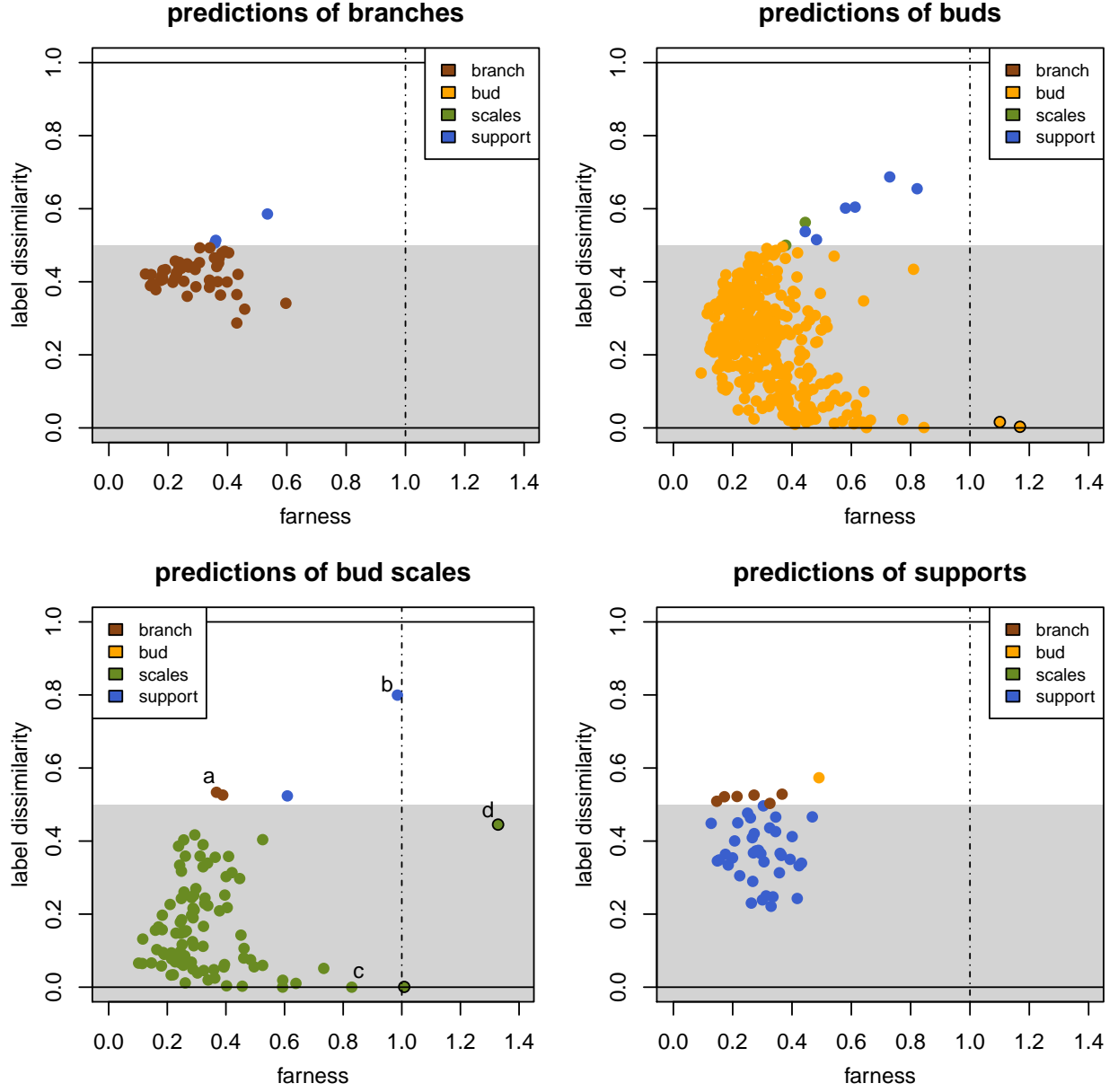


Figure 3: Floral buds data: maps of all four classes.

We now illustrate class maps on the benchmark data set of USPS digits due to Le Cun et al. (1990). It contains 7291 images of handwritten digits, ranging from 0 to 9, which were automatically scanned from envelopes by the U.S. Postal Service. Each image has been deslanted and normalized to a size of  $16 \times 16$  pixels on a grayscale. The top row of Figure 4 shows some randomly sampled images from the dataset, one of each digit, and the bottom row shows the averaged image per class.



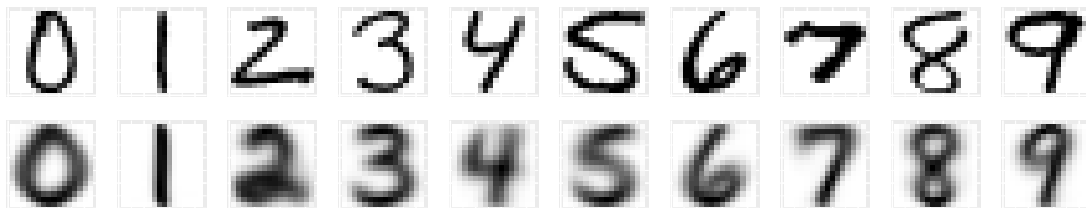


Figure 4: Top row: randomly sampled digits; bottom row: averaged images per class.

To predict digits from images we first reduced the dimension of the data from 256 to 100 using PCA. These 100 principal components explain roughly 98% of the total variance which is enough to obtain a solid classification performance while avoiding numerical instability due to the inversion of covariance matrices in QDA.

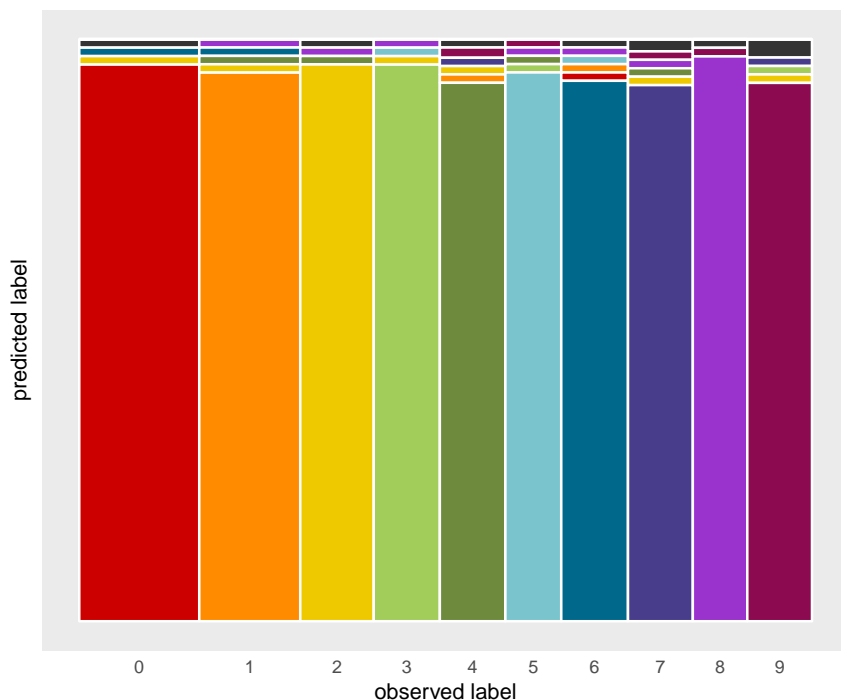


Figure 5: Digits data: stacked plot where the objects flagged as outliers are shown in dark grey, as an extra class at the top.

The misclassification rate of QDA on these data is quite low, around 1.3%. Figure 5 is the stacked mosaic plot of the QDA classification. Unlike Figure 1, here we opted to see the overall fairness outliers, given by  $O(i) > 1$  in (6), as an extra predicted class in dark grey at the top. Fortunately there are not many outliers here. The largest fraction of outliers

is found in the images of digit 9 (top right).

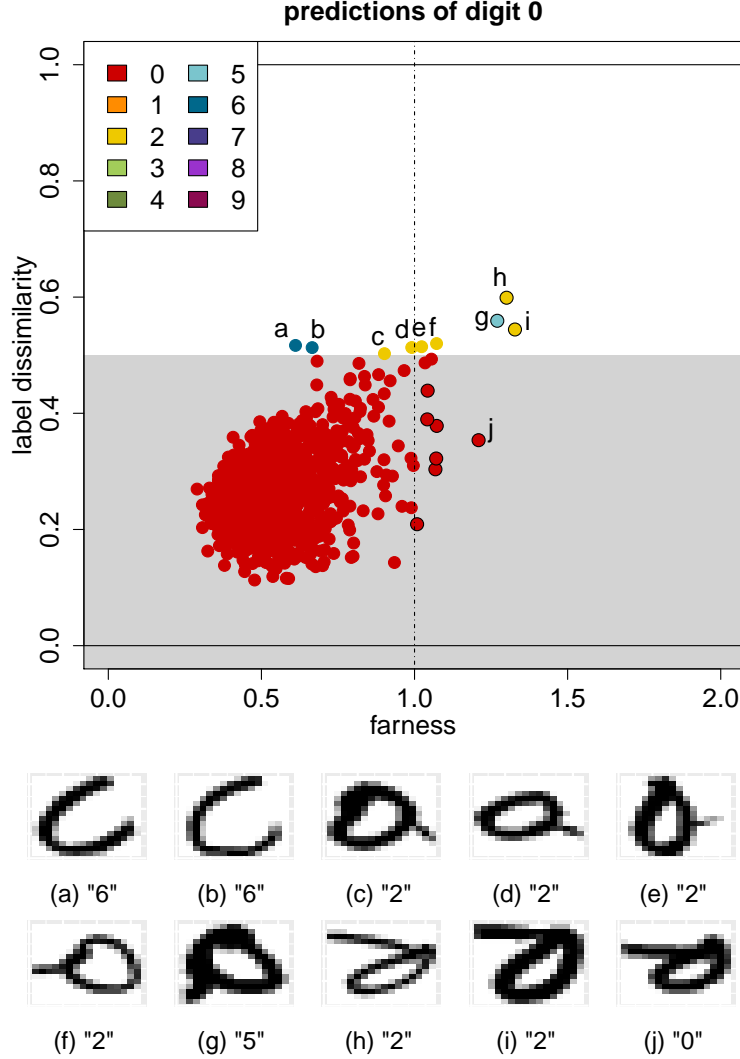


Figure 6: Class map of the digit 0, with the images corresponding to the labeled points.

The top panel of Figure 6 is the class map of the digit 0. Most points have a low label dissimilarity LD, meaning they are well within the class. The labeled points stand out, and the corresponding images are shown below it. Let us start with the points above the grey zone, that is, whose predictions differ from 0. The LD of most of them is just barely above 0.5, so they are merely borderline cases. Points **a** and **b** are predicted as 6, which is not surprising when looking at their images. The other points with  $LD > 0.5$  have the shape of a ring with an extra penstroke. QDA predicts most of them as 2, and indeed they bear some similarity to the average 2 in the bottom row of Figure 4. Image **g** is considered

closer to a 5. Points g, h, i and j have a black border, meaning they do not sit comfortably in any class. Point j does fall in the grey zone so it was correctly predicted as 0, but still its image does not look like a clean digit 0.

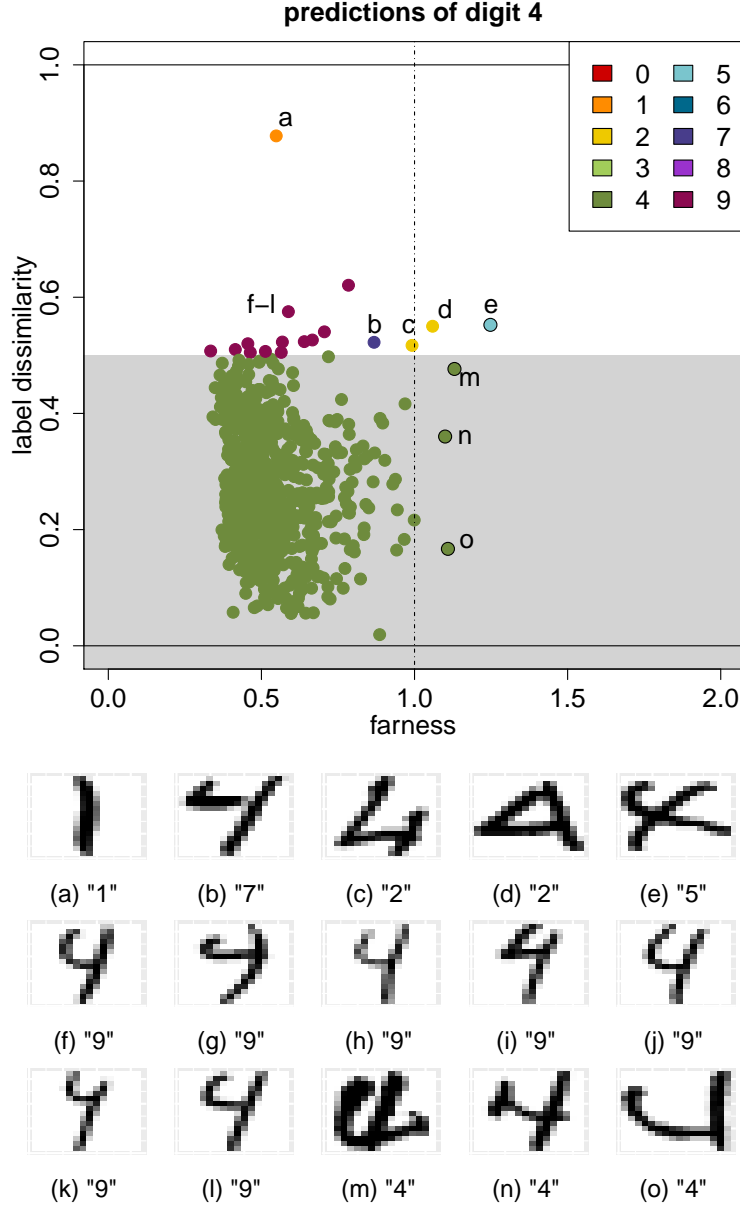


Figure 7: Class map of the digit 4, with the images corresponding to the labeled points.

The class map of digit 4 in Figure 7 is also quite interesting. Point a has by far the highest LD so it is predicted in a different class with substantial conviction. And indeed its image looks a lot like 1. The LD of points b and c is just barely above 0.5, with images

still looking like a 4. Images **d** and **e** look less like a 4, and in the class map they have a higher LD as well as a higher farness. Points **f** to **l** are predicted as 9, due to the top part of their images tending to close. And finally points **m** to **o** are predicted correctly but have a somewhat high farness, and indeed their images are rather sloppy versions of 4.

The class maps of the remaining eight digits as well as the relevant images can be found in Section A.1 of the Supplementary Material.

## 4 Classification by k-nearest neighbors

Another popular classifier is the *k-nearest neighbor method* (kNN) of Cover and Hart (1967), which has several appealing properties. It is not restricted to data points with coordinates, as it can take data in the form of dissimilarities  $d(i, j)$  between objects. Such a dissimilarity matrix may for instance originate from subjective judgments, in which case there were no coordinates to begin with, and the axioms of a metric need not be satisfied. Of course, if there are coordinates one can always compute dissimilarities from them. This even works when the variables are of mixed types. Chapter 1 of (Kaufman and Rousseeuw, 1990) describes how one can compute a dissimilarity matrix from mixed variables of continuous, symmetric binary, asymmetric binary, nominal and ordinal types, and this is implemented in the function `daisy()` of the R package `cluster` (Maechler et al., 2019).

Around each object  $i$  the kNN method determines its *k-neighborhood* consisting of the objects  $j \neq i$  with the  $k$  smallest  $d(i, j)$ . Let us denote the  $k$ -th such dissimilarity as  $d_i^*$ . Such a neighborhood is not always unique, as it can happen that there are other objects  $j'$  with the same dissimilarity  $d(i, j') = d_i^*$ . To make the neighborhood unique a common option is to include such points  $j'$  as well, so we get neighborhoods  $N(i)$  with  $k(i)$  members where always  $k(i) \geq k$ .

In  $N(i)$  we define the relative frequency of a class (label)  $g$  as

$$\xi_i(g) := n_i(g)/k(i) \tag{7}$$

where  $n_i(g)$  counts how many objects in the neighborhood have label  $g$ . In general  $0 \leq \xi_i(g) \leq 1$  with both endpoints occurring. The kNN classifier then predicts the label of  $i$  as the class  $\hat{g}_i$  with highest  $\xi_i(g)$ . Also here ties can occur. Some implementations choose

randomly between tied labels. Our implementation breaks ties by assigning  $i$  to the tied label  $g$  for which the average dissimilarity between  $i$  and the members of  $g$  in  $N(i)$  is lowest.

From its definition we see that kNN makes no explicit assumptions about underlying distributions, and that it can focus on local structure (nearby objects) rather than global structure. Both aspects are quite different from DA. For a given dataset, a typical way to select an appropriate value of  $k$  is to cross validate the misclassification rate. Here we will assume that  $k$  has already been selected.

For the label dissimilarity we use the kNN criterion  $\varphi(i, g) = \xi_i(g)$  and compute  $\tilde{\varphi}(i)$  and  $\Delta(i)$  from (1) and (2). But whereas  $\Delta(i)$  ranged over the entire real line in discriminant analysis, for kNN its range is only  $[-1, 1]$ . This makes it easy to normalize, yielding the label dissimilarity

$$\text{LD}(i) = (\Delta(i) + 1)/2 \tag{8}$$

with values in  $[0, 1]$ . Here the end points can be attained exactly:  $\text{LD}(i) = 0$  implies that all the members of  $N(i)$  have the same label  $g_i$ . At the other extreme,  $\text{LD}(i) = 1$  says that all the members of  $N(i)$  have the same label  $\hat{g}_i$  which differs from  $g_i$ . The boundary is again at  $\text{LD} = 0.5$ , with  $\text{LD}(i) > 0.5$  signifying that the predicted label  $\hat{g}_i$  fits better than the given label  $g_i$ . Unlike DA here  $\text{LD}(i)$  takes discrete values, with steps of size  $1/k(i)$ .

For computing farness we can no longer use (5) since the kNN classifier does not require coordinates. For each object  $i$  and class  $g$  we instead compute  $f(i, g)$  as the median of the  $k$  smallest dissimilarities  $d(i, j)$  to objects  $j$  of class  $g$ . Note that these  $d(i, j)$  will often be larger than those in the neighborhood  $N(i)$ . For each class  $g$  we then replace all  $f(i, g)$  for  $i = 1, \dots, n$  by  $f(i, g)/\text{median}\{f(j, g); j = 1, \dots, n\}$ . This makes the farness values from all classes more comparable to each other. Finally, we compute a cutoff value by transforming the farness values to central normality (as we did for DA), and divide the farness values by their cutoff so the new cutoff value is 1. The overall farness outliers are then identified by (6) as before.

We illustrate the resulting display on the benchmark *spam* data. These consist of 4601 emails collected by George Forman at the Hewlett-Packard Labs, and are labeled as spam (1813 mails) or non-spam (2788 mails). The data is publicly available in the R-package **kernlab** (Karatzoglou et al., 2004). The mails were converted to a numerical

characterization using 57 variables. Section A.2 of the Supplementary Material lists the variables and their interpretation. Unfortunately, the mails themselves are not available.

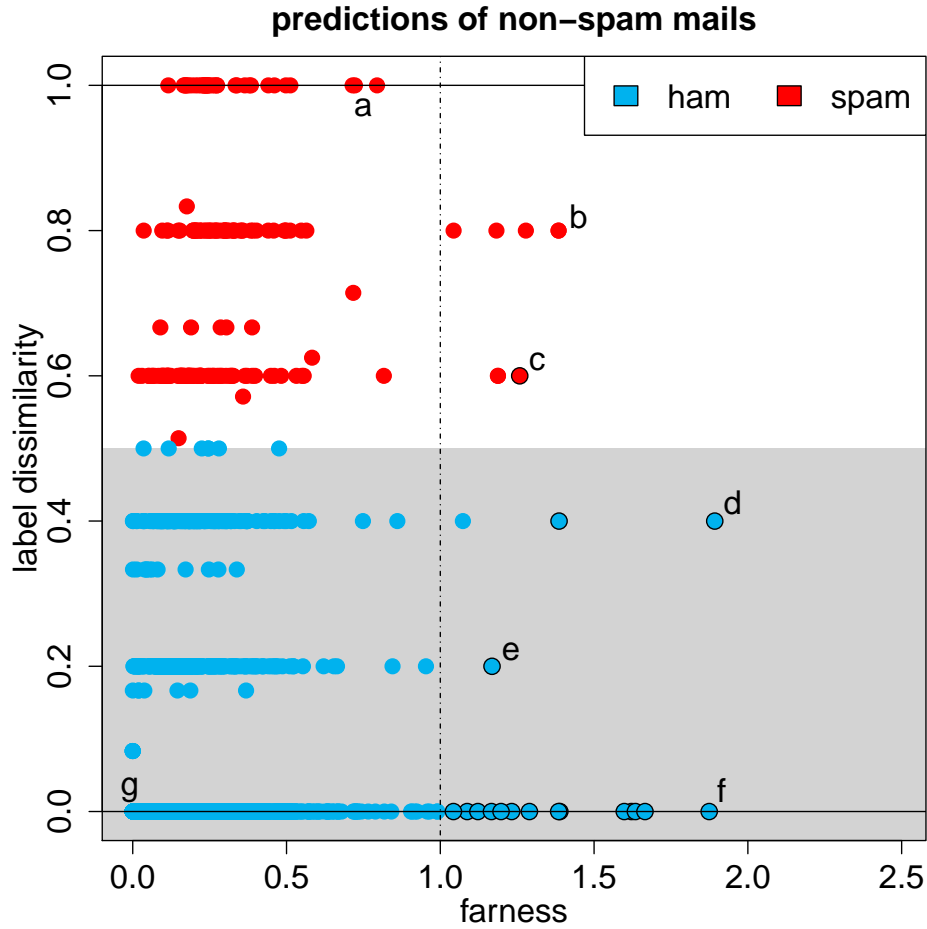


Figure 8: Class map of the non-spam mails.

The data are classified by kNN with  $k = 5$ , yielding an in-sample misclassification rate under 9%. Figure 8 shows the class map of the non-spam (also called ham) mails. As expected, most of the LD values are at one of the six main levels between  $LD = 0$  and  $LD = 1$  by steps of  $1/k = 0.2$ . The LD values in between these levels come from the neighborhoods  $N(i)$  that contain  $k(i) > k$  members due to tied dissimilarities.

Some atypical points are labeled. Point **a** has maximal  $LD = 1$  so it is strongly predicted as spam. It corresponds to a mail containing 1506 capitalized characters, 1488 of which in a single string. Capitalization is more common in spam messages, explaining why it was predicted as spam. Point **b** is a mail of which 20% consists of the word ‘free’. This word

is more common in spam mails, so its frequent occurrence makes the mail suspicious. In mail **c**, 7.5% of the characters are ‘#’ which appears more often in spam mails than in non-spam, and 7.5% is the highest percentage in any non-spam mail.

The next points are correctly predicted as non-spam. Point **d** has a high farness because 30% of its characters are exclamation marks, but it also contains some non-spam features such as a high frequency of ‘re’ (since spam mails are usually not replies). Mail **e** has no special characteristics except for the highest frequency of the word ‘report’. Mail **f** is classified perfectly with  $LD = 0$  but has a high farness because it contains the number 85 much more often than any other mail in the dataset. This number is characteristic for the non-spam class however, since it occurs in all the telephone and fax numbers of the HP labs, including those of the person collecting the data. Finally, **g** corresponds with a mail that has no particularly extreme values except for a 20% frequency of the word ‘george’, the name of the collector. This explains its low farness and low (good) LD.

Figure 9 is the class map of the spam messages. Also here some points stand out. Mail **h** has  $LD = 1$  so the classifier predicted it as non-spam with high conviction. It has a very high frequency of the round bracket character, typically associated with non-spam mails. Similarly, mail **i** also contains many round brackets, in addition to the word ‘technology’. On the other hand it also has an extreme number of ‘#’ symbols (indicative of spam) which explains its high farness. Mail **j** contains a string of 9989 capitalized characters. This causes it to be correctly classified as spam, but it also gets a high farness. Similarly, mail **k** is perfectly (since  $LD = 0$ ) classified as spam, but has a high farness as well. It contains a very high frequency (almost 20%) of the word ‘credit’. This is a common word in spam messages, but 20% is unusually high.

## 5 Support vector machines

A support vector machine (SVM) is based on a kernel. Starting from a training set with  $n$  objects, the kernel matrix  $K$  is of the form  $\{K(i, j); i = 1, \dots, n \text{ and } j = 1, \dots, n\}$ . The values  $K(i, j)$  play the role of inner products, unlike the entries of the dissimilarity matrix in the kNN method which played the role of distances. The kernel may be derived from a coordinate data set  $\{\mathbf{x}_1, \dots, \mathbf{x}_n\}$ . Many kernel functions exist for that situation.

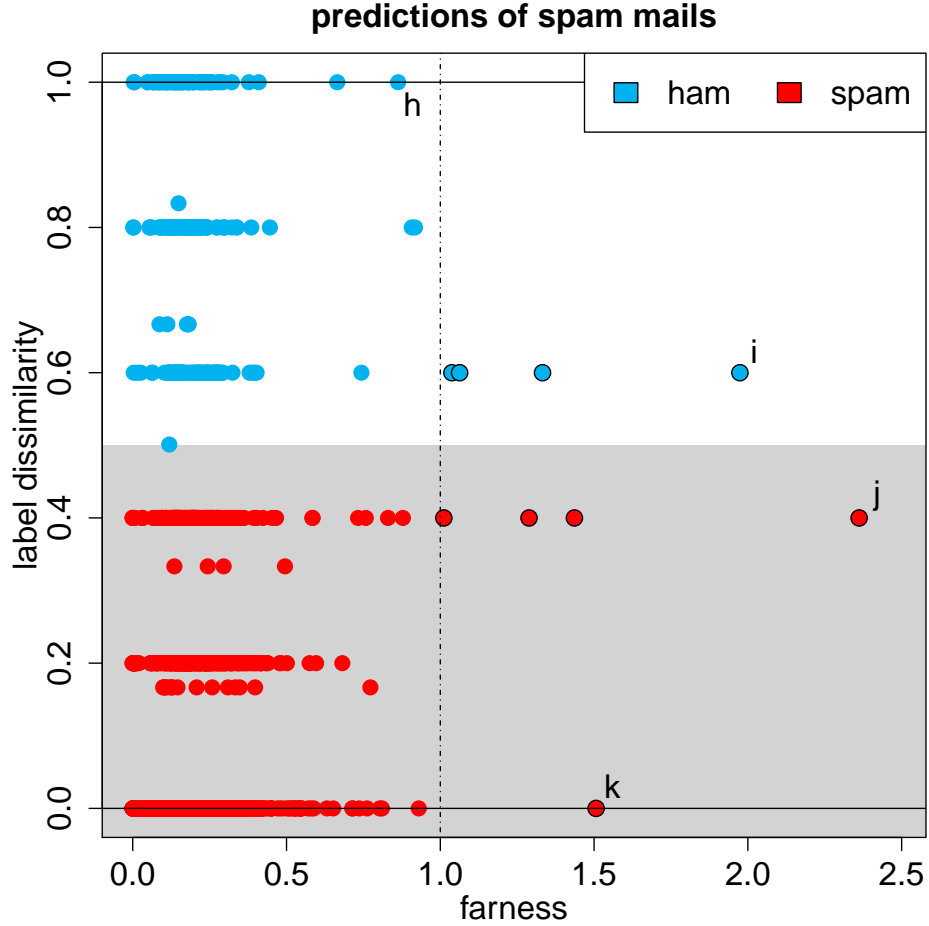


Figure 9: Class map of the spam mails.

The linear kernel is just  $K(i, j) = \langle \mathbf{x}_i, \mathbf{x}_j \rangle$  where  $\langle \cdot, \cdot \rangle$  is the usual inner product. The polynomial kernel is  $K(i, j) = (\gamma \langle \mathbf{x}_i, \mathbf{x}_j \rangle + c)^{\text{degree}}$  with tuning constants  $\gamma$ ,  $c$  and the degree. The radial basis kernel is given by  $K(i, j) = \exp(-\gamma \|\mathbf{x}_i - \mathbf{x}_j\|^2)$ . Each of these can be seen as  $K(i, j) = \langle \Phi(\mathbf{x}_i), \Phi(\mathbf{x}_j) \rangle$  where  $\Phi(\cdot)$  maps the original data to a feature space. For the linear kernel we can just take  $\Phi(\mathbf{x}) = \mathbf{x}$  so there is no transformation. The other two kernels have a feature space of a higher dimension than the original space, in fact for the radial basis kernel that dimension is even infinite. However, the feature space is often left implicit since all computations can be carried out on the kernel matrix  $K$  itself. An advantage of kernels is the added flexibility, as it is often easier to separate classes in a higher dimensional feature space than in the original space.

The SVM applies the support vector (SV) classifier in feature space, i.e. to data  $\mathbf{v} =$



$\Phi(\mathbf{x})$ . The SV classifier is a method for  $G = 2$  classes which looks for a linear boundary that separates the classes as well as possible. This is achieved by an optimization with a tuning constant `cost` that determines to what extent some points are allowed to be poorly classified. The value of `cost` is typically selected by cross-validation to avoid overfitting. The end result is an estimated vector  $\hat{\boldsymbol{\beta}}$  and intercept  $\hat{\beta}_0$  yielding the prediction

$$\hat{g}(\mathbf{v}) = \begin{cases} 1 & \text{if } \hat{\beta}_0 + \langle \mathbf{v}, \hat{\boldsymbol{\beta}} \rangle > 0 \\ 2 & \text{if } \hat{\beta}_0 + \langle \mathbf{v}, \hat{\boldsymbol{\beta}} \rangle \leq 0. \end{cases} \quad (9)$$

One often calls  $\hat{\beta}_0 + \langle \mathbf{v}, \hat{\boldsymbol{\beta}} \rangle$  the decision value. Note that also classification by linear discriminant analysis (LDA) is in function of a quantity  $\hat{\beta}_0 + \langle \mathbf{v}, \hat{\boldsymbol{\beta}} \rangle$  but it is not the same as it derives from a different optimization.

We can rewrite the assignment rule (9) as maximizing the criterion

$$\varphi(i, g) = (\hat{\beta}_0 + \langle \mathbf{v}_i, \hat{\boldsymbol{\beta}} \rangle)(1.5 - g) \quad (10)$$

using the midpoint 1.5 of  $g = 1, 2$ . We then obtain  $\tilde{\varphi}(i)$  and  $\Delta(i)$  from (1)–(2). Since  $\Delta(i)$  can be any real number, we compute the label dissimilarity by (4) as in discriminant analysis, with values in  $[0, 1]$ . The interpretation of LD remains the same as before.

Farness needs to be defined in relation to how the classifier works. The SVM tries to linearly separate the points in the feature space. Since the kernel matrix is invariant to multiplying the  $\mathbf{v}_i$  by an orthogonal matrix, also the farness needs to be. Orthogonally equivariant linear structures suggests using principal component analysis (PCA). Since the PCA must be applied in the feature space it is, in fact, kernel PCA (KPCA), but here we will write everything in terms of the feature vectors  $\mathbf{v}_i$ .

Carrying out a PCA on the  $\mathbf{v}_i$  in class 1 yields an estimated center  $\hat{\boldsymbol{\mu}}_1$  of class 1, a matrix  $\hat{\mathbf{U}}_1$  with the loadings in its columns, and scores  $\mathbf{t}_i = (\mathbf{v}_i - \hat{\boldsymbol{\mu}}_1)\hat{\mathbf{U}}_1$  for all  $i = 1, \dots, n$ . Here we keep all components, so the scores  $\mathbf{t}_i$  have the same dimension as the space  $\mathbf{V}_1$  spanned by the  $\mathbf{v}_i$  in class 1. We then compute the *score distance* of any object  $i$  relative to class 1 as

$$\text{SD}(i, 1) = \sqrt{\sum_j \left( \frac{t_{ij} - \text{median}_h(t_{hj})}{\text{mad}_h(t_{hj})} \right)^2} \quad (11)$$

where  $\text{mad}$  is the median absolute deviation. In this formula  $h$  ranges over the members of class 1, whereas  $i$  can belong to either class. We compute  $\text{SD}(i, 2)$  analogously.

When the spaces  $\mathbf{V}_1$  and  $\mathbf{V}_2$  are equal, the score distances are all we need. Otherwise,  $\mathbf{V}_1$  and/or  $\mathbf{V}_2$  is a proper subset of the space  $\mathbf{V}$  spanned by the  $\mathbf{v}_i$  of both classes together. This often happens when using the radial basis kernel because then the dimension of  $\mathbf{V}$  can be very high (but not infinite). In such situations a point  $\mathbf{v}_i$  of class 1 may not be in  $\mathbf{V}_2$ . We then compute how far  $\mathbf{v}_i$  is from  $\mathbf{V}_2$  by the euclidean distance between  $\mathbf{v}_i$  and its projection on  $\mathbf{V}_2$  given by

$$\text{OD}(i, 2) = \|\mathbf{v}_i - (\hat{\boldsymbol{\mu}}_2 + (\mathbf{v}_i - \hat{\boldsymbol{\mu}}_2)\hat{\mathbf{U}}_2\hat{\mathbf{U}}_2')\| \quad (12)$$

which is called the *orthogonal distance*.

Next we have to combine the score and orthogonal distances into a single fairness measure. For this we first scale all  $\text{SD}(i, g)$  by the median of the  $\text{SD}(i_g, g)$  where  $i_g$  ranges over the  $i$  in class  $g$ . Next we scale all  $\text{OD}(i, g)$  by the median of the  $\text{OD}(i_g^*, g)$  where  $i_g^*$  ranges over all  $i$  *not* belonging to class  $g$  (since  $\text{OD}(i, g) = 0$  when  $i$  belongs to  $g$ ). Then the fairness  $f(i, g)$  of an object  $i$  to a class  $g$  is given by

$$f(i, g) = \sqrt{\text{SD}^2(i, g) + \text{OD}^2(i, g)} \quad (13)$$

Finally we compute a cutoff value for the  $f(i, g)$  as in DA, and divide all  $f(i, g)$  by that cutoff so the new cutoff value is 1, in line with the previous sections.

Note that SVM can also be applied to  $G > 2$  classes by means of the majority voting technique. Since majority voting is also used with other classifiers, it will be discussed separately in Section 7.

We illustrate the class maps for SVM on a benchmark data set in which the data do not originate from coordinates (measurements). It is one of the datasets collected and studied by Prettenhofer and Stein (2010) and consists of 4000 book reviews on Amazon written in English. The reviews were binned into two categories: positive (with 4 or more stars out of 5) and negative (under 3 stars). The 4000 reviews were split up, the first 2000 forming the training set and the next 2000 the test set.

The data are actual texts, some of them quite long. The kernel matrix was constructed by a string kernel, in fact the function `kernlab::stringdot()` with `type="spectrum"` and

`length=7`. Afterward the SVM was trained with parameter `cost=2` using the R-package `e1071` (Meyer et al., 2019). The combination of `length` and `cost` was selected by 10-fold cross validation.

On the training data itself the SVM seems to overfit quite strongly, with not a single misclassified book review. (Perhaps this is not so surprising since kernel PCA requires as many as 1804 components to explain 95% of the variance, so we are in a truly high dimensional setting.) Since not much label dissimilarity is visible in the training data, its class maps are relegated to Section A.3 of the Supplementary Material. On the test data, the trained SVM obtained a correct classification rate of 82%.

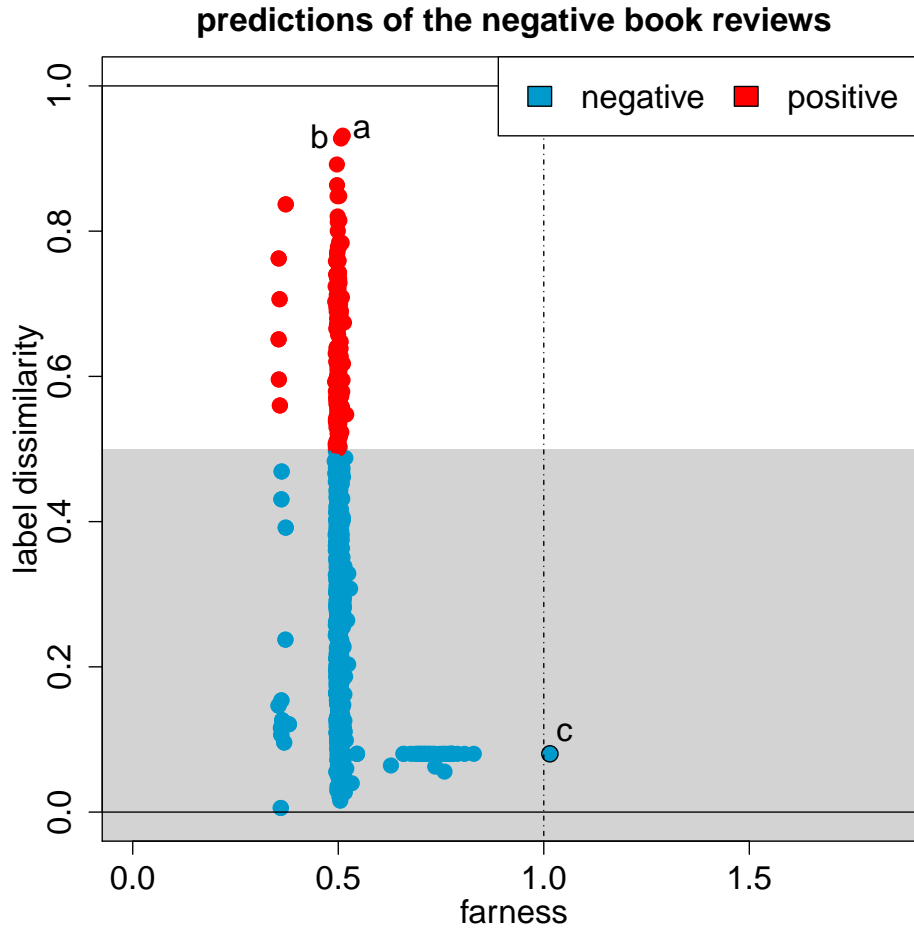


Figure 10: Class map of the negative book reviews in the test data.

The class map of the negative reviews is shown in Figure 10. Many points, but not all, lie in a thick vertical band. This is not always the case, it has to do with the high effective

Table 1: Excerpts of the negative reviews **a**, **b** and **c**.

label	excerpts from the book reviews
<b>a</b>	“ptt may well be one of heinein’s masterworks” “this collection looses the continuity that made the ptt a great read”
<b>b</b>	“i have liked his other books in the past” “this one didn’t have enough insight”
<b>c</b>	“read ‘as nature made him’ by john colapint”

dimensionality of the data set. About 80% of these reviews were correctly classified as negative (blue). Let’s look at some points that stand out. Reviews **a** and **b** have the highest LD. Excerpts of these reviews are in Table 1. Why was it so hard to classify them correctly? Review **a** has both positive and negative elements. The reviewer is positive about the author and the stories, but negative about the selection of stories presented in this particular book. Review **b** is similar in that it praises the author and his past works, but is negative about the current book. Review **c** is a one-sentence review (the excerpt in Table 1 is in fact the complete review) that is neutral and uninformative, which may explain its relatively high farness from both classes.

The class maps of the positive reviews in the test data are in Figure 11. Also here some points stand out from the others. Book review **d** has the lowest farness. It is a very positive review, as illustrated by the excerpt in Table 2. Review **e** has the highest LD indicating that the classifier strongly wanted to put it in the negative class. It is nevertheless a positive review, but not unequivocally so since it also indicates for which purposes you should not use this book. Book review **f** is correctly predicted as positive, but has a very high farness. It turns out to be in Spanish, whereas the reviews in this dataset are supposedly all in English. The high farness value is a result of the Spanish words not matching well with the English words in the other reviews.

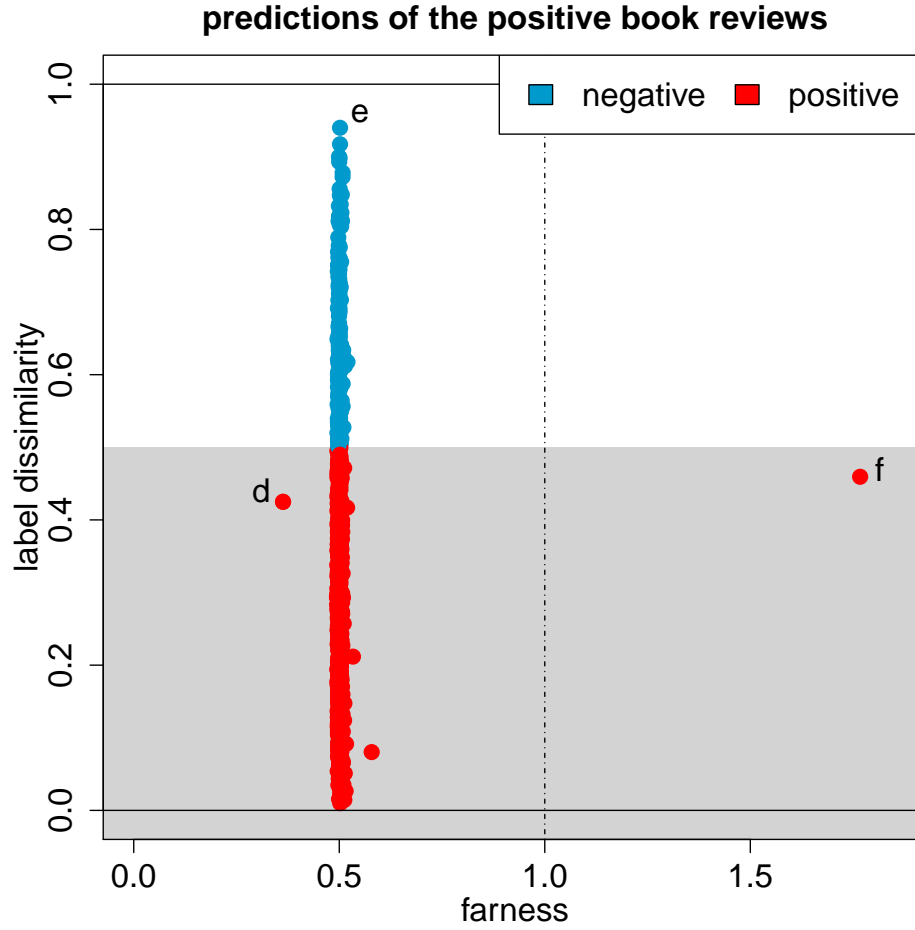


Figure 11: Class map of the positive book reviews in the test data.

Table 2: Test data: Excerpts from the positive reviews **d**, **e** and **f**.

label	excerpts from the book reviews
<b>d</b>	“i moved through it at a steady pace” “the character development was outstanding”
<b>e</b>	“i have not found any other c++ reference that is as complete or as useful as this books” “this is not an introduction to c++ but rather a reference book”
<b>f</b>	“cosmos es un libro acerca de la vida” “es un libro lento pero rico en descripciones”

## 6 Logistic regression

In the context of logistic regression the classes are typically denoted as 0 and 1 (instead of 1 and 2 as in the other sections), so we are predicting a binary variable  $y$ . The coordinates of the  $\mathbf{x}_i$  can be continuous as well as binary. The logistic model assumes that the response has probability  $\pi_i$  to be 1 and  $1 - \pi_i$  to be 0, with  $\pi_i = \text{logist}(\beta_0 + \langle \mathbf{x}_i, \boldsymbol{\beta} \rangle)$ . Here  $\text{logist}(z) = \exp(z)/(1 + \exp(z))$  is the logistic function, and the unknown parameters  $\beta_0$  and  $\boldsymbol{\beta}$  are typically estimated by maximum likelihood, yielding  $\hat{\beta}_0$  and  $\hat{\boldsymbol{\beta}}$ . Each object then obtains the predicted probability

$$\hat{\pi}_i = \text{logist}(\hat{\beta}_0 + \langle \mathbf{x}_i, \hat{\boldsymbol{\beta}} \rangle) . \quad (14)$$

Object  $i$  is assigned to the class closest to  $\hat{\pi}_i$ , so the class  $g$  minimizing  $|g - \hat{\pi}_i|$ . Since our formulas assume that we maximize a criterion, we put

$$\varphi(i, g) = -|g - \hat{\pi}_i| . \quad (15)$$

Then  $\Delta(i) = \tilde{\varphi}_i - \varphi(i, g_i) = \varphi(i, 1 - y_i) - \varphi(i, y_i) = -|(1 - y_i) - \hat{\pi}_i| + |y_i - \hat{\pi}_i| = -1 + |y_i - \hat{\pi}_i| + |y_i - \hat{\pi}_i| = 2|y_i - \hat{\pi}_i| - 1$  with range  $[-1, 1]$ . Normalizing it by (8) yields

$$\text{LD}(i) = |y_i - \hat{\pi}_i| \quad (16)$$

with range  $[0, 1]$  and the same interpretation as in the other sections.

The fairness measure we use depends on the dimensionality of the regressors  $\mathbf{x}_i$ . If the dimension is low we can use the fairness as in Section 3 on discriminant analysis, which is based on the Mahalanobis distance. We have the choice between estimating a single  $\hat{\boldsymbol{\Sigma}}$  for both classes as in linear DA, or separate  $\hat{\boldsymbol{\Sigma}}_0$  and  $\hat{\boldsymbol{\Sigma}}_1$  as in quadratic DA. In either case the fairness is invariant to affine transformations of the  $\mathbf{x}_i$ , just like the  $\hat{\pi}_i$  of logistic regression itself and therefore also the level dissimilarity  $\text{LD}(i)$ . Note that for linear regression we can replace (16) by the residual  $y_i - \hat{y}_i$  which recovers the outlier map of Rousseeuw and van Zomeren (1990), later extended to multivariate regression (Rousseeuw et al., 2004).

When the  $\mathbf{x}_i$  are high dimensional one may prefer to run sparse logistic regression, for instance using the R-package `glmnet` (Friedman et al., 2020). Since sparse logistic regression does not have the affine invariance property we can then compute fairness as in Section 5 on support vector machines.

## 7 Majority voting

When the data has  $G > 2$  labels but the preferred classifier was designed for 2 labels (like the support vector machine), one often resorts to ‘one versus one’ majority voting. In this approach one carries out a binary classification on each pair of classes, yielding  $C := G(G - 1)/2$  comparisons. Any object  $i$  thus obtains votes for each class  $g$ , let us denote their number as  $N_i(g)$ . Clearly  $0 \leq N_i(g) \leq G - 1$  where the upper bound is because each class  $g$  is compared to the  $G - 1$  remaining classes. The total number of votes is  $\sum_{g=1}^G N_i(g) = C$ . Majority voting assigns  $i$  to the class  $\hat{g}_i$  with the highest number of votes, which we denote as  $\hat{N}_i := \max\{N_i(g); i = 1, \dots, G\}$ .

The assignment criterion being maximized is thus  $\varphi(i, g) = N_i(g)$ . Applying (1) and (2) immediately yields  $\tilde{\varphi}(i) = \tilde{N}_i$  and

$$\Delta(i) = \tilde{N}_i - N_i \quad (17)$$

where  $N_i$  is short for  $N_i(g_i)$ . Finding an appropriate normalization is a bit more complex in this setting. If  $\Delta(i) > 0$  we know that  $N_i < \tilde{N}_i = \hat{N}_i$  so object  $i$  will not be assigned to label  $g_i$ . Then  $0 < \Delta(i) \leq \hat{N}_i$  where the upper bound can be reached, which happens when the given label  $g_i$  got zero votes. So using (8) we can put

$$\text{LD}(i) = \left( \frac{\tilde{N}_i - N_i}{\tilde{N}_i} + 1 \right) / 2 \quad \text{when} \quad N_i < \tilde{N}_i \quad (18)$$

which is in  $]0.5, 1]$ .

When instead  $\tilde{N}_i - N_i \leq 0$  it is not immediately clear what the lower bound is on  $\tilde{N}_i - N_i$ . Note that  $\tilde{N}_i$  cannot be zero, as the total number of votes would then be less than  $C$ . Along the same lines we can show that always  $\tilde{N}_i \geq \lceil G/2 \rceil - 1$ . Assume the opposite, that is  $\tilde{N}_i \leq \lceil G/2 \rceil - 2$ . Then the total number of votes is  $\sum_{g=1}^G N_i(g) \leq (G - 1) + \sum_{g \neq g_i} (\lceil G/2 \rceil - 2) = (G - 1) + (G - 1)(\lceil G/2 \rceil - 2) = (G - 1)(\lceil G/2 \rceil - 1) < (G - 1)G/2 = C$ , a contradiction. From this it follows that  $\tilde{N}_i - N_i \geq \lceil G/2 \rceil - 1 - (G - 1) = \lceil G/2 \rceil - G = -\lfloor G/2 \rfloor$ . (It can also be verified that this lower bound is sharp.) Therefore, we can put

$$\text{LD}(i) = \left( \frac{\tilde{N}_i - N_i}{\lfloor G/2 \rfloor} + 1 \right) / 2 \quad \text{when} \quad N_i \geq \tilde{N}_i \quad (19)$$

using (8), yielding a value in  $[0, 0.5]$ . The range of  $\text{LD}(i)$  given by the combination of (18) and (19) is thus the interval  $[0, 1]$ , and it is interpreted in the usual way.

For drawing class maps we also need a measure of farness. For this we can use one of the methods described in the earlier sections. If the data have continuous coordinates and the dimension is not too high, we can compute the Mahalanobis distance as in (5) which is affine invariant. If the data has coordinates of mixed types or is given in the form of a dissimilarity matrix we can run the same farness computation as for the  $k$ -nearest neighbor method in Section 4. And if we have high-dimensional continuous data or the input is a kernel matrix, we can apply formulas (11)–(13) yielding an orthogonally invariant farness measure.

As an illustration of majority voting we analyze the sweets data. This is a subset of the `nutrients_branded` dataset which is publicly available in the R-package `robCompositions` (Templ et al., 2020). It contains data on 9 nutritional values of 804 different sweets sold in Switzerland, which are divided into 4 categories: ‘Cookies and Biscuits’, ‘Milk based ice cream’, ‘Cakes and tarts’, and ‘Creams and puddings’. The nutritional variables are the contents of energy (kcal), protein, water, carbohydrates, sugars, dietary fibers, total fat, saturated fatty acids, and salt.

We used the function `svm()` in the R-package `e1071` (Meyer et al., 2019) with linear kernel. The parameter `cost=10` was selected by 10-fold cross-validation, yielding a misclassification rate of 13%. We used farness measure (13). Figure 13 shows the maps of all classes, whose names were abbreviated to ‘biscuits’, ‘ice cream’, ‘cakes’, and ‘puddings’.

Figure 12 shows the stacked mosaic plot of this classification. We see at a glance that puddings (the yellow stack at the right) are often predicted as pink, the color of the stack of ice cream. Unlike Figure 1, here the option to show the overall farness outliers is switched on. They are visible as an extra predicted class in dark grey at the top for those classes where they occur.

The class maps in Figure 13 contain a lot of structure. Not being experts in nutrition, we have only labeled the atypical points we can say something about. The names of the objects `a` to `u` are listed in Section A.4 of the Supplementary Material.

Let’s start with the biscuits. Point `a` has the highest LD. It corresponds to a kind of gingerbread, and is predicted as a cake due to its low energy level and relatively high water content. Point `b` has  $LD = 0.5$  so it is on the fence. It is a coconut biscuit with low protein



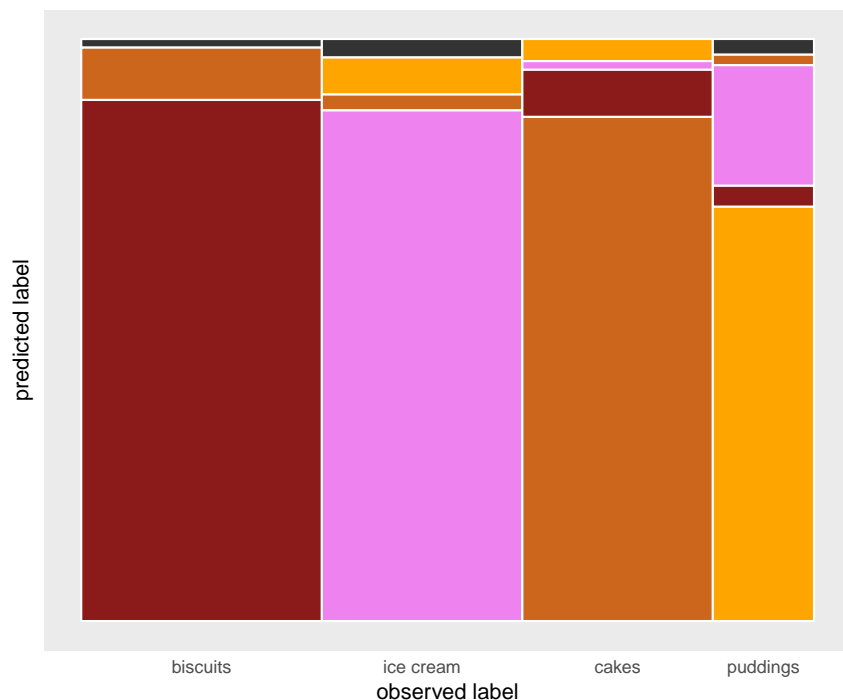


Figure 12: Sweets data: Stacked mosaic plot of the classification. The products flagged as outliers are now shown in dark grey, as an extra class at the top, where they occur.

and high water content. It has in fact received 2 votes for cake and 2 votes for ice cream. Note that the function `svm()` is based on the library LIBSVM of Chang and Lin (2019) who say on page 30 that in the case of such a tie the class is chosen which appears first in the list of levels (here this is ‘biscuits’). One could think of other tie-breaking mechanisms, but the graphical display has to show what the actual classifier does.

Among the ice creams, **c** and **d** are produced by Burger King and have a high level of salt. Product **c** is predicted as pudding and **d** as cake, perhaps because of its high protein content which is more common in cakes. Products **e** and **f** have a high LD and a high farness. Both are predicted as pudding, but their black border circles indicate that they are far from every class. It turns out that **e** and **f** are Weight Watchers products, with exceptionally high levels of dietary fibers and low sugars. Finally, the ice creams **g** and **h** are classified correctly but also far from each class. They are also dietary products with high fiber and low sugar levels.

In the class map of cakes object **i** is predicted as ice cream, but is in fact a strawberry

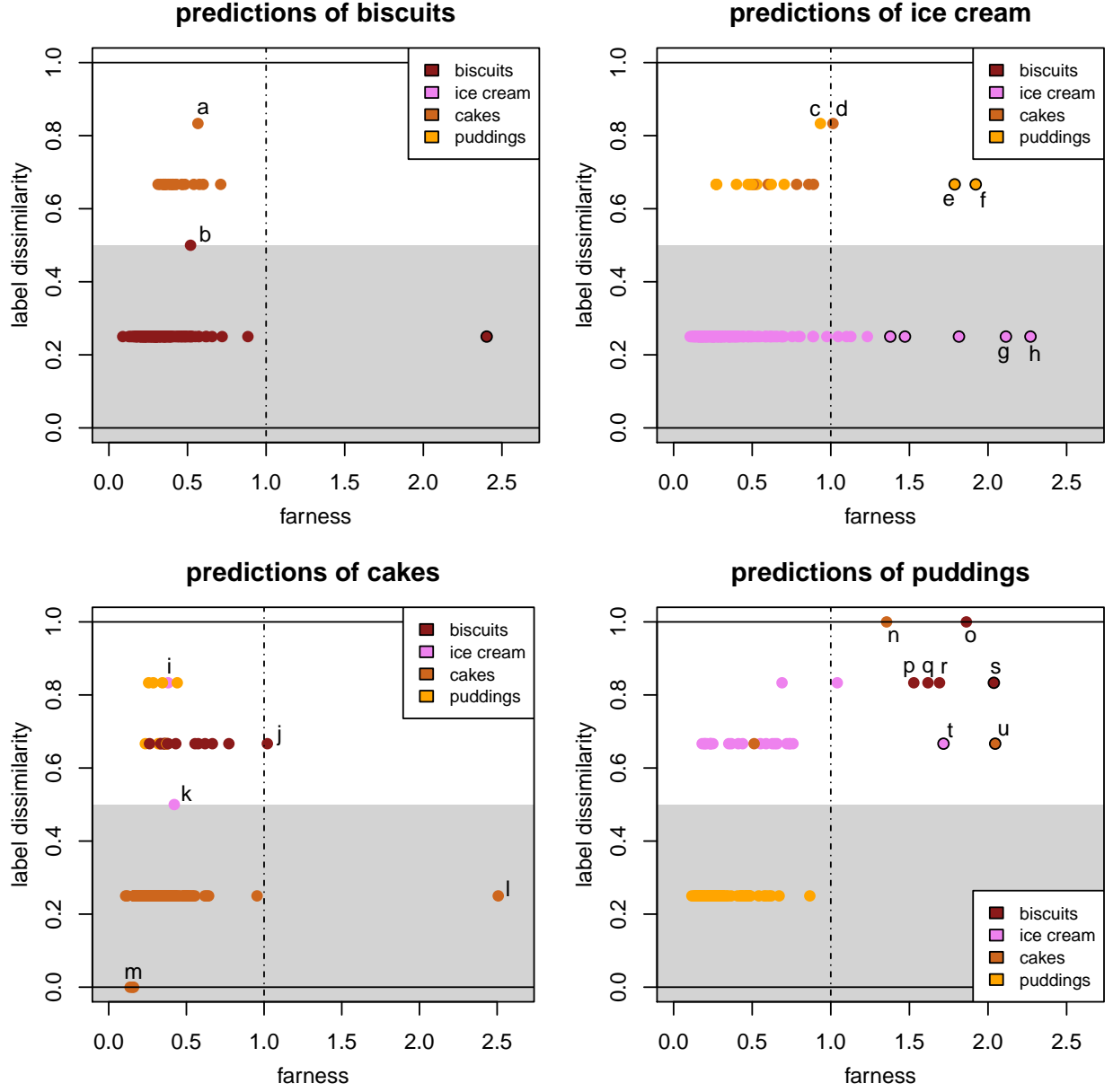


Figure 13: Class maps of all four classes in the sweets data.

tart with high water content and low sugar. Point **j** is a carrot cake with high protein and fibers, and predicted as a biscuit. Object **k** has  $LD = 0.5$  as it sits on the fence between cake and ice cream, perhaps due to its low calorie, protein and fat contents combined with high water content. Cake 1 is classified correctly but quite far from its class, it has a liquid inside which is unusual. Finally, point **m** reaches the lowest  $LD = 0$ , which in the case of majority voting with  $G = 4$  means that cake got 3 votes and all other classes only a single

vote each. Cake **m** is thus well within its given class.

Among the puddings, point **n** has the maximal  $LD = 1$  and is predicted as a cake. Nearly all of its nutritional values are exceptional for pudding but normal for cake. On the store website it looks like a small chocolate cake, so it may actually have been mislabeled. The puddings labeled **o-s** have a high  $LD$  and are all predicted as biscuits. In fact, they are dry mixes (powders) to make pudding at home. They have extremely low water content (since this is an ingredient that needs to be added to the mix), which makes them more similar to biscuits. Product **t** is a dry mix for sugar free pudding, and is predicted in the class of ice cream that has the lowest average sugar level of the four classes. Finally, **u** is a dark chocolate mousse with extreme levels of salt (the highest in the whole dataset). High salt levels are more common for cakes than for puddings so the product is classified as a cake, but we see that it is far from every class.

## 8 Conclusions

The proposed graphical display reflects two basic notions. In the vertical direction it shows the dissimilarity of the given label to the prediction, which is analogous to the absolute residual in regression analysis. And in the horizontal direction we see how far the object is from its given class, with a separate plotting symbol when it is far from all classes.

This visualization often provides useful information, as illustrated on data classified by discriminant analysis, k-nearest neighbors, support vector machines, and majority voting. Further research is underway to extend this approach to other classifiers such as neural nets.

**Software availability.** The R code and an example script reproducing all the figures in this paper, as well as the data sets required, can be downloaded from the website <https://wis.kuleuven.be/statdatascience/robust/software>.

**Acknowledgement.** This research was funded by projects of Internal Funds KU Leuven.

# References

- Chang, C.-C. and C.-J. Lin (2019). *LIBSVM: A Library for Support Vector Machines*. National Taiwan University.
- Cover, T. and P. Hart (1967). Nearest neighbor pattern classification. *IEEE Transactions on Information Theory IT-11*, 21–27.
- Friedman, J., T. Hastie, R. Tibshirani, B. Narasimhan, K. Tay, and N. Simon (2020). *Package glmnet: Lasso and Elastic Net Regularized Generalized Linear Models*. CRAN, R package version 4.0-2.
- Friendly, M. (1994). Mosaic displays for multi-way contingency tables. *Journal of the American Statistical Association* 89, 190–200.
- Hartigan, J. and B. Kleiner (1981). Mosaics for contingency tables. In *Computer Science and Statistics: Proceedings of the 13th Symposium on the Interface*, New York, pp. 268–273. Springer.
- Hastie, T., R. Tibshirani, and J. Friedman (2017). *The Elements of Statistical Learning: Data Mining, Inference, and Prediction, 12th printing*. Springer Series in Statistics.
- Karatzoglou, A., A. Smola, K. Hornik, and A. Zeileis (2004). **kernlab** – an S4 package for kernel methods in R. *Journal of Statistical Software* 11(9), 1–20.
- Kaufman, L. and P. Rousseeuw (1990). *Finding Groups in Data: An Introduction to Cluster Analysis*. Wiley-Interscience, Hoboken, New Jersey.
- Le Cun, Y., O. Matan, B. Boser, J. S. Denker, D. Henderson, R. E. Howard, W. Hubbard, L. Jacket, and H. S. Baird (1990). Handwritten zip code recognition with multilayer networks. In *Proceedings of 10th International Conference on Pattern Recognition*, Volume 2, pp. 35–40. IEEE.
- Maechler, M., P. J. Rousseeuw, A. Struyf, and M. Hubert (2019). *cluster*. CRAN, R package version 2.1.0.

- McLachlan, G. J. (2004). *Discriminant Analysis and Statistical Pattern Recognition*. Wiley-Interscience, Hoboken, USA.
- Meyer, D., E. Dimitriadou, K. Hornik, A. Weingessel, and F. Leisch (2019). *e1071*. CRAN, R package version 1.7-3.
- Prettenhofer, P. and B. Stein (2010). Cross-language text classification using structural correspondence learning. In *Proceedings of the 48th Annual Meeting of the Association for Computational Linguistics*, pp. 1118–1127.
- Raymaekers, J. and P. J. Rousseeuw (2020). Transforming variables to central normality. arXiv:2005.07946v1.
- Rousseeuw, P. J. (1987). Silhouettes: a graphical aid to the interpretation and validation of cluster analysis. *Journal of Computational and Applied Mathematics* 20, 53–65.
- Rousseeuw, P. J., S. Van Aelst, K. Van Driessen, and J. Agulló (2004). Robust multivariate regression. *Technometrics* 46, 293–305.
- Rousseeuw, P. J. and B. van Zomeren (1990). Unmasking multivariate outliers and leverage points. *Journal of the American Statistical Association* 85, 633–651.
- Templ, M., K. Hron, and P. Filzmoser (2020). *robCompositions: an R-package for robust statistical analysis of compositional data*. CRAN, R package version 2.2.1.
- Wouters, N., B. De Ketelaere, T. Deckers, J. D. Baerdemaeker, and W. Saeys (2015). Multispectral detection of floral buds for automated thinning of pear. *Computers and Electronics in Agriculture* 113, 93–103.

# A Supplementary Material

## A.1 More on the USPS data

Figure 14 shows the farness of each image from its own class, binned by class (digit). Second from left is digit 1, whose farness has the longest tail. We will see that this class indeed has an interesting class map.

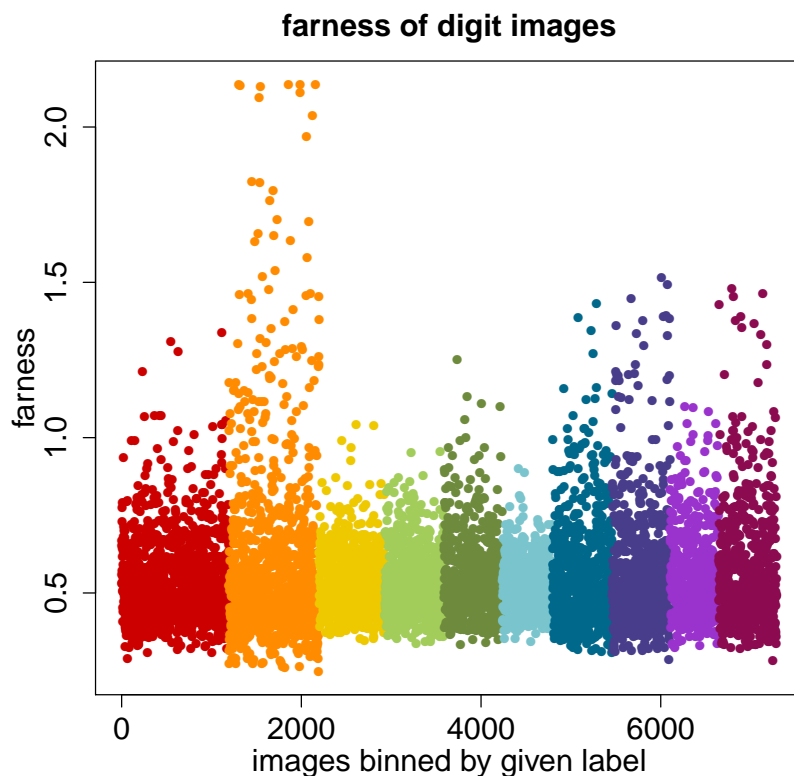


Figure 14: Digits data: farness of each image from its given class, binned by class.

The class map of digit 1 is in Figure 15. Out of the 1005 images, QDA predicts 15 in a different class. These are the points above the grey region. The shape of this class map is unusual, since here increasing LD go together with increasing farness. To understand why, note that the average image of the digit 1 (in the bottom row of Figure 4) is a thin vertical line which is much sharper than the other average digits, so the images of 1 are more concentrated around their average. As a result, images deviating from this simple

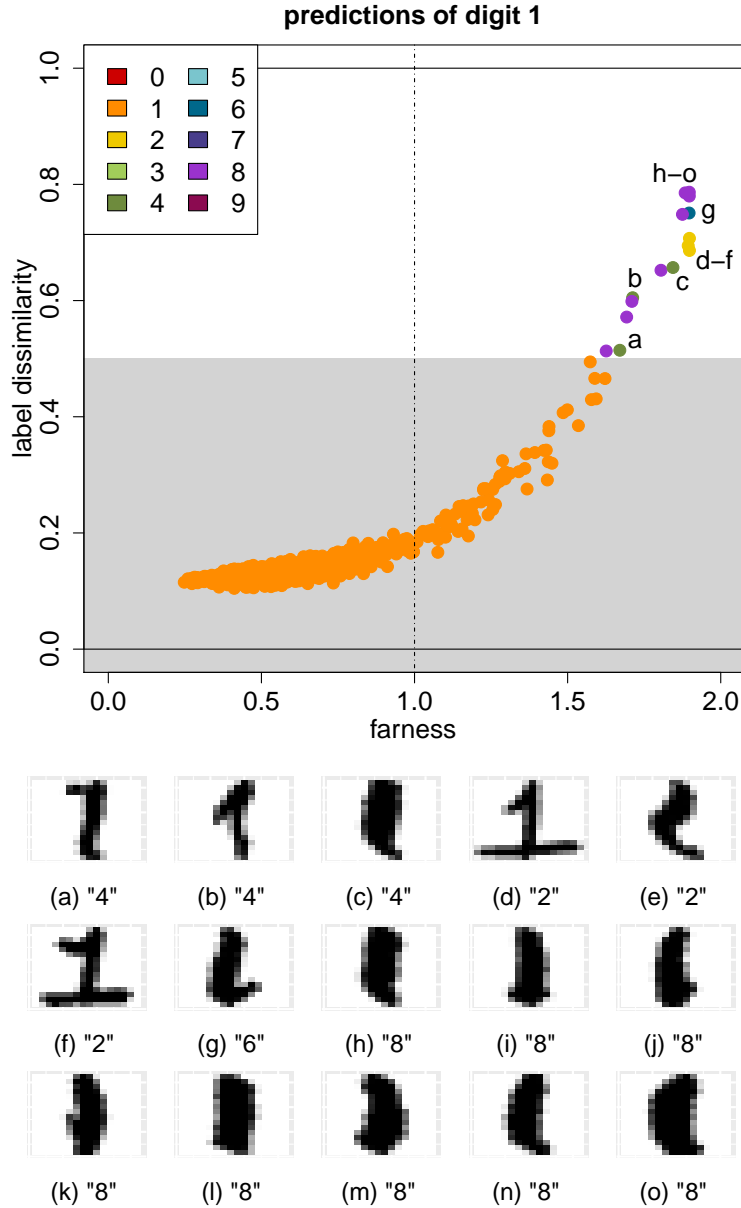


Figure 15: Class map of digit 1, with the images corresponding to the labeled points. Images a, b, c and e have sloppy writing. Images d and f are predicted as 2 due to their horizontal lines. Digit g has a curly shape and is predicted as 6. The images labeled h-o are considered too thick for a 1 and predicted as 8. All of the labeled points also have a high farness, suggesting that they are in the outskirts of their class.

shape will be considered very different from it which gets reflected in a high farness, and at the same time they will tend to get a prediction different from 1.

This explains for instance why the points in the upper right corner labeled **h-o** have a high farness because they are considered way too thick to be a 1, causing them to be predicted as the wider image 8 even though they are missing the “holes” of an 8. Images **d** and **f** both contain a horizontal line and are the only images of 1 that do, as we can verify in Figure 16 which shows all images of 1 in the entire data set. It is therefore understandable that the classifier predicts **d** and **f** as 2, whose average image does have a horizontal line. Image **g** looks curly and is predicted as 6. The images **c** and **e** are sloppily written, and we would argue that even a human might struggle with their classification.



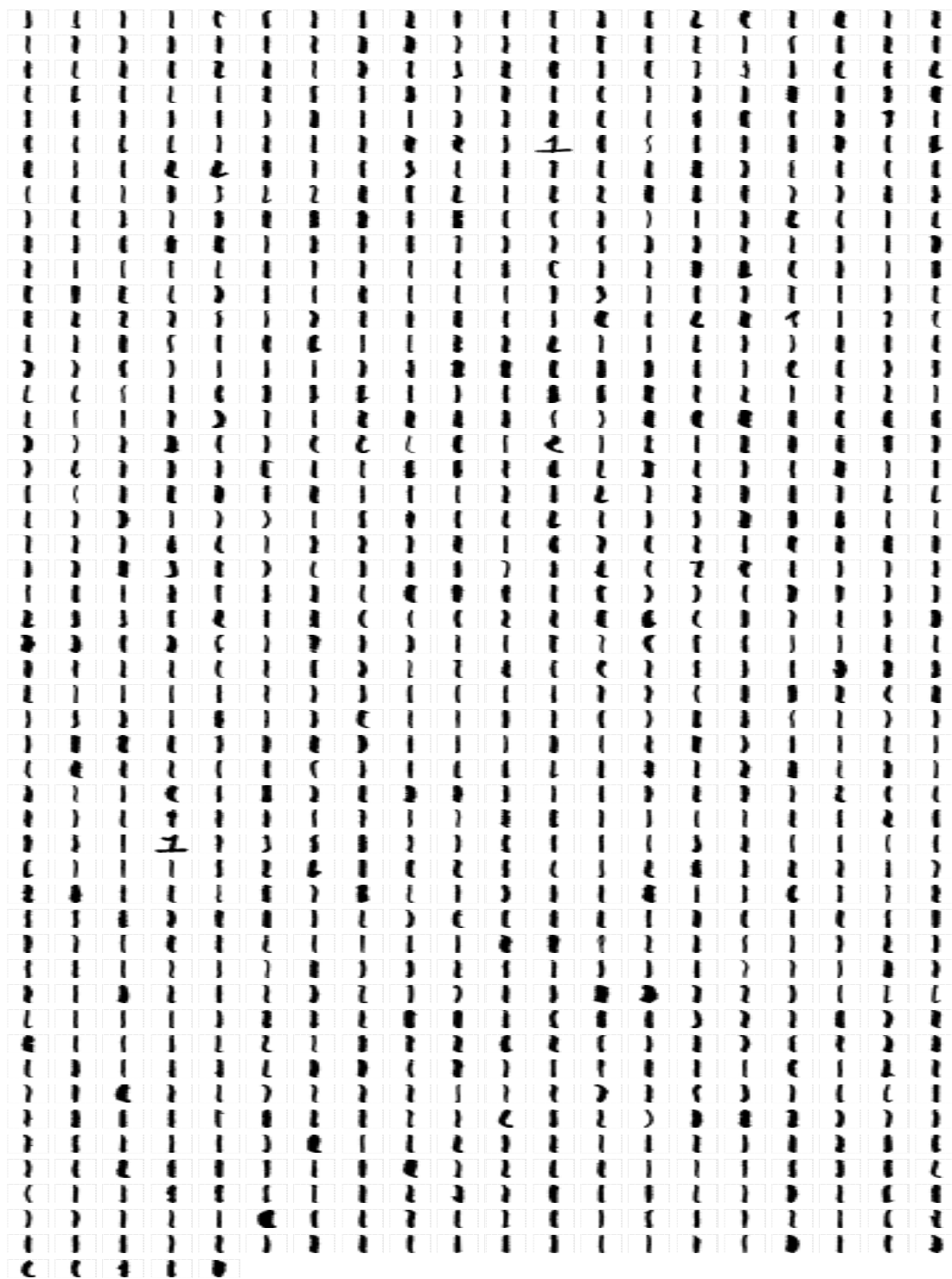


Figure 16: All the images of the digit 1 in the data.

Figure 17 shows the class map of digit 2, in which many points have a favorably low LD. Out of the 731 images of this digit the class map suggests only 5 that deviate, and just barely, which indicates that the classifier captures the shape of this digit very well. Three points have a label dissimilarity above 0.5. Two of these, labeled **a** and **b**, are considered to be closer to the digit 4. The other, labeled **c**, is predicted as 8. In the corresponding images we see that **a** and **b** look like a 4 that is missing a vertical penstroke, and **c** looks like half of the digit 8. There are also two points in the grey zone that lie slightly to the right of the fairness cutoff, so they are merely borderline cases. They correspond to the images **d** and **e** which are sloppily written but do not really look like any other digit.

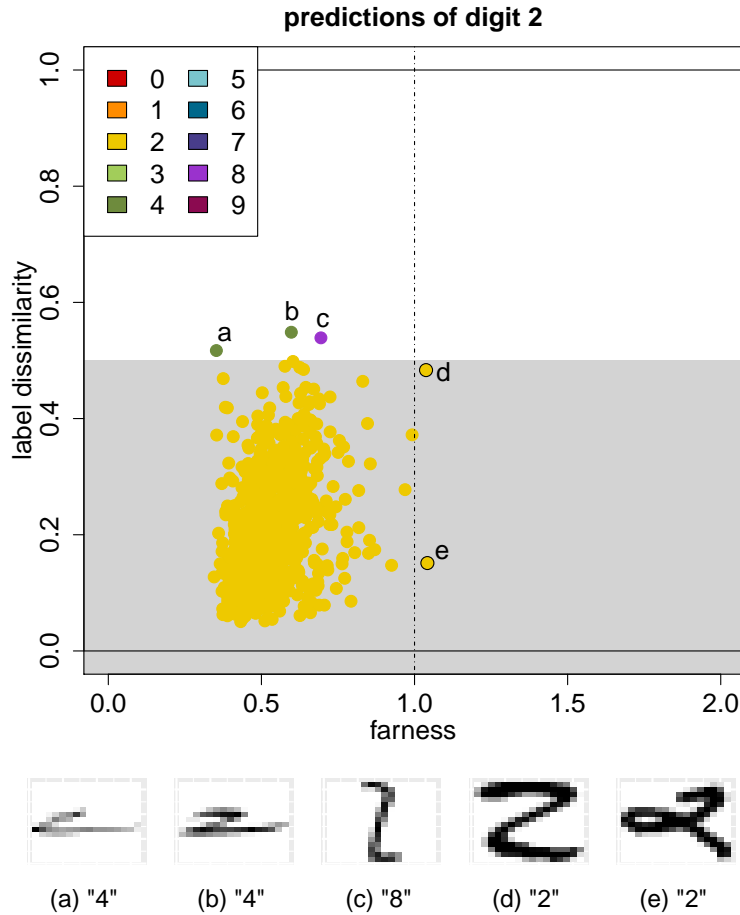


Figure 17: Class map of digit 2, with the images corresponding to the labeled points.

Figure 18 shows that the digit 3 is also well classified by QDA. There are no points with high farness, and only 9 with  $LD > 0.5$ . Image **a** is considered closer to a 5, and images **b** to **g** are predicted as 8. While a human would probably classify **a–g** correctly as 3, we see that their shapes deviate from the averaged 3 in Figure 4. In particular, the bottom part of **b**, **c** and **d** is almost a closed circle as in an 8. Finally, images **h** and **i** look like a 2 and a 3 written on top of each other, explaining why they are predicted as 2.

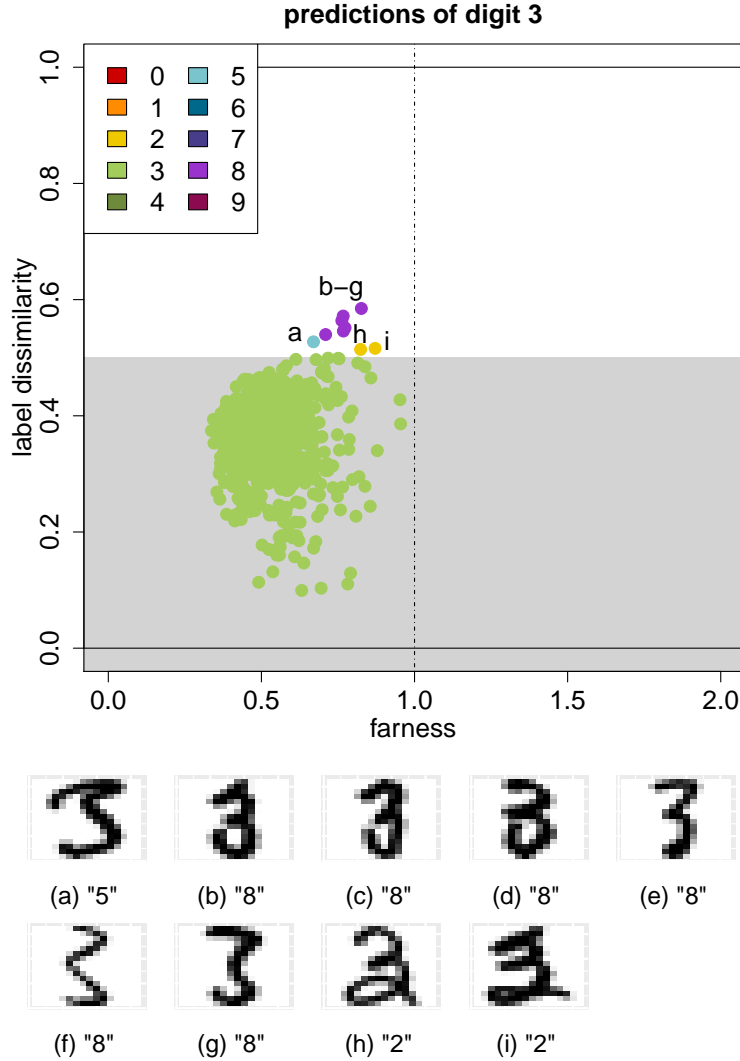


Figure 18: Class map of digit 3, with the images corresponding to the labeled points.

The class maps of the remaining digits are shown next. Most of them are self-explanatory, but we can say a bit more about digit 7 in Figure 19. That class map contains quite a few points with  $LD > 0.5$  and/or high farness, suggesting that the digit 7 is relatively hard to

classify. Images a–d look like a question mark and are considered closer to 9. Digits e–g are thinly written and predicted as 4. Several other images are predicted as 2, 4, and 8. Finally, the points in the grey zone to the right of the dashed line are predicted correctly as 7 but poorly written, like s and t.

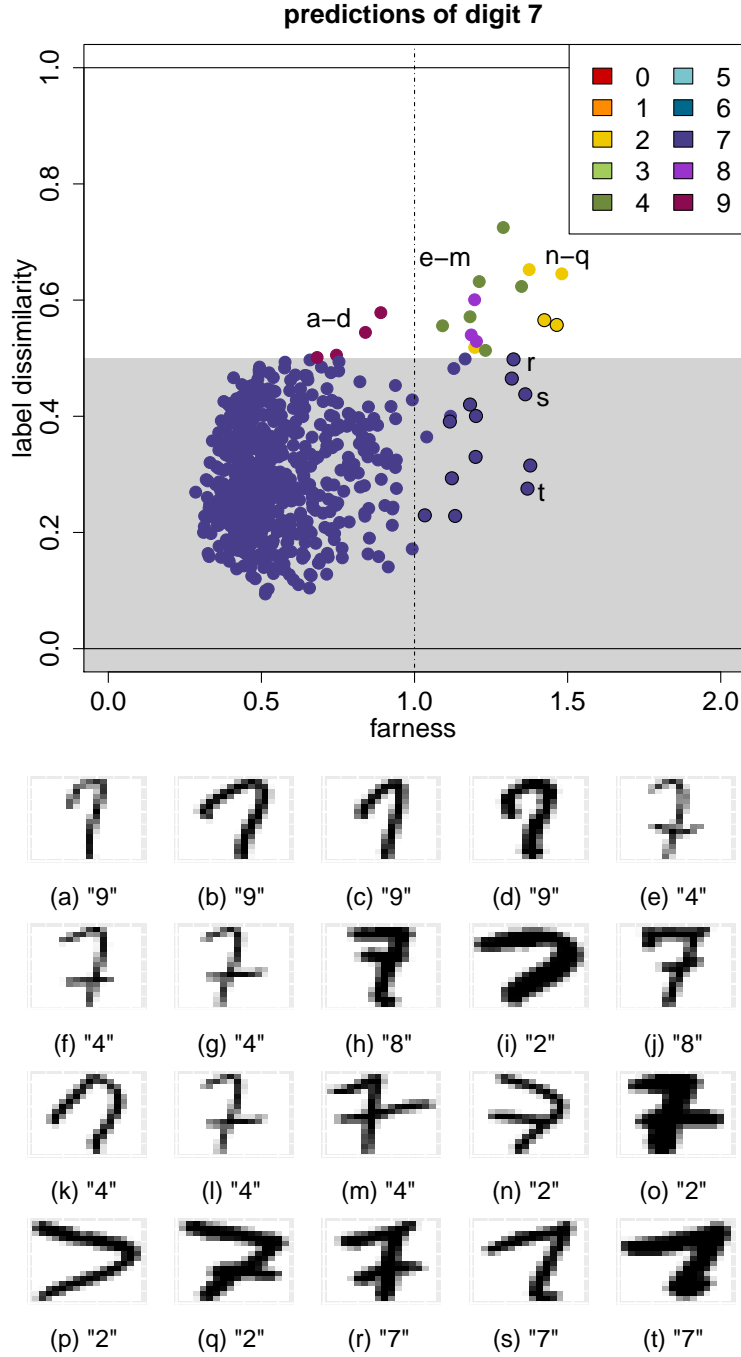


Figure 19: Class map of digit 7, with the images corresponding to the labeled points.

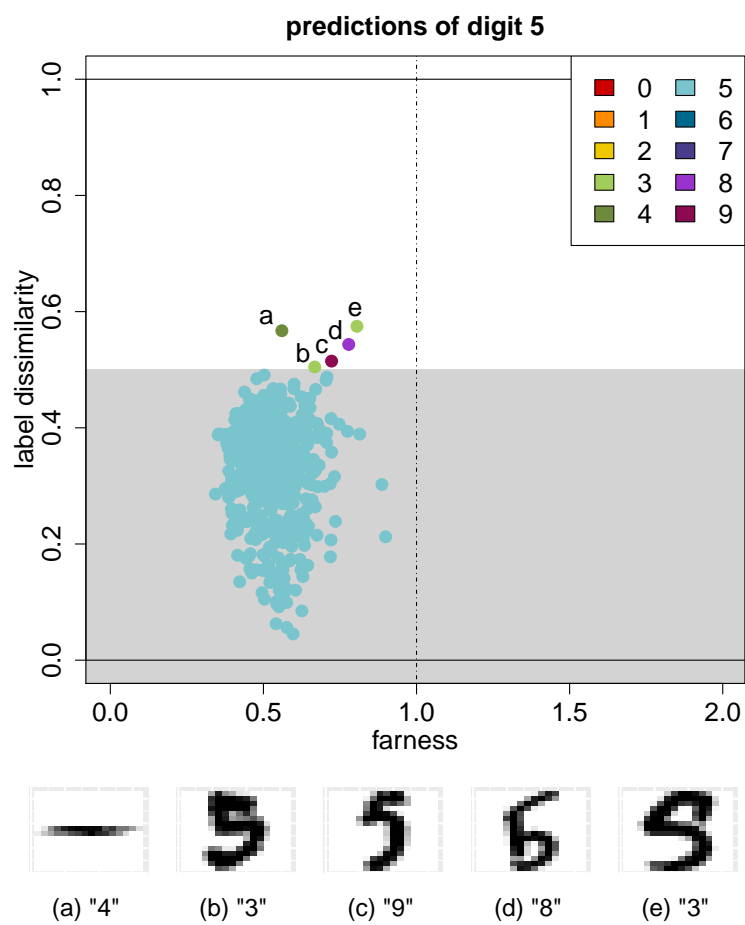


Figure 20: Class map of digit 5, with the images corresponding to the labeled points.

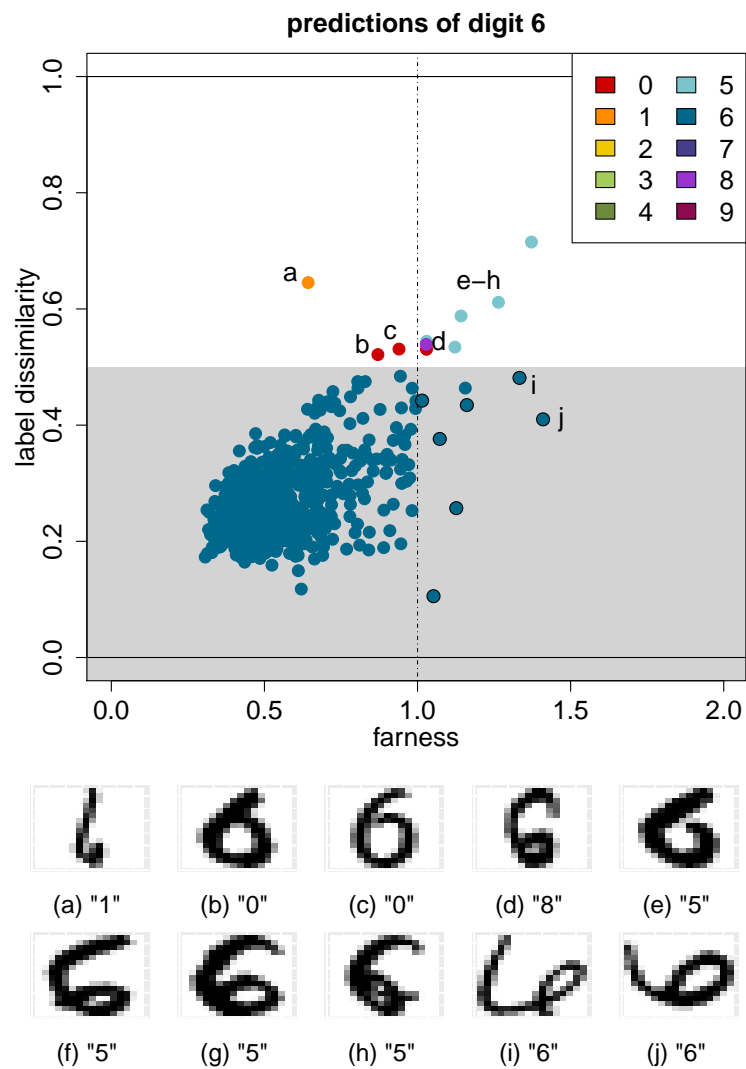


Figure 21: Class map of digit 6, with the images corresponding to the labeled points.

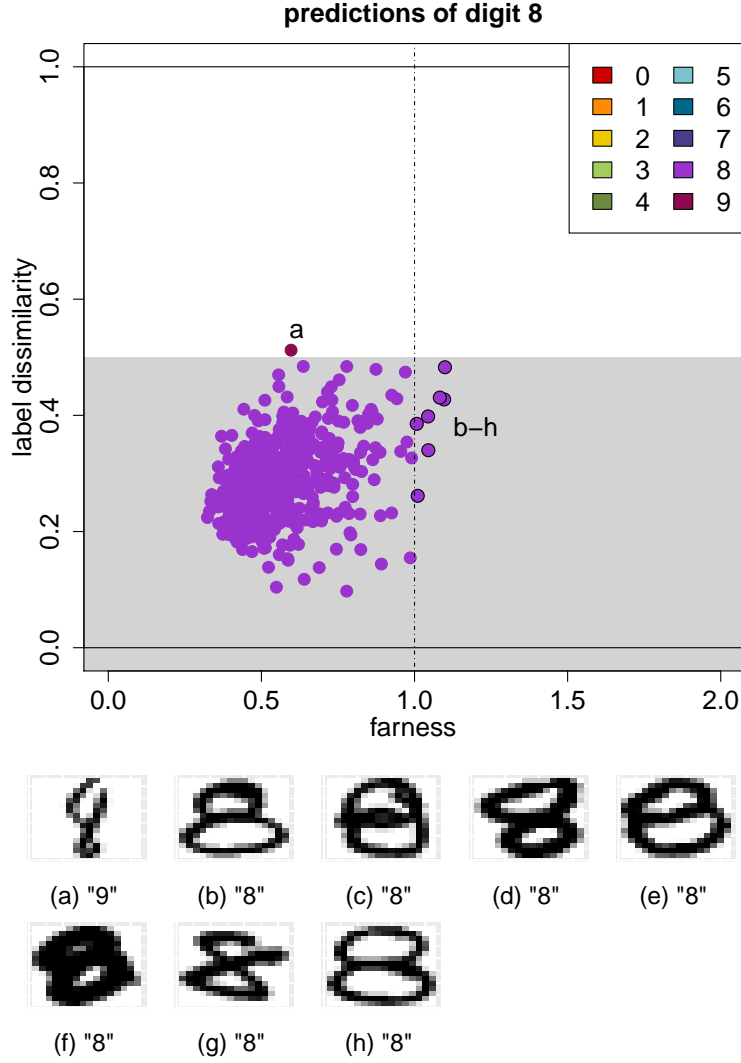


Figure 22: Class map of digit 8, with the images corresponding to the labeled points. Point a has  $LD > 0.5$  and corresponds to a poorly written 8 with characteristics of a 9. Points b–h are predicted correctly but their farness is slightly high. The corresponding images are wider than the average 8.

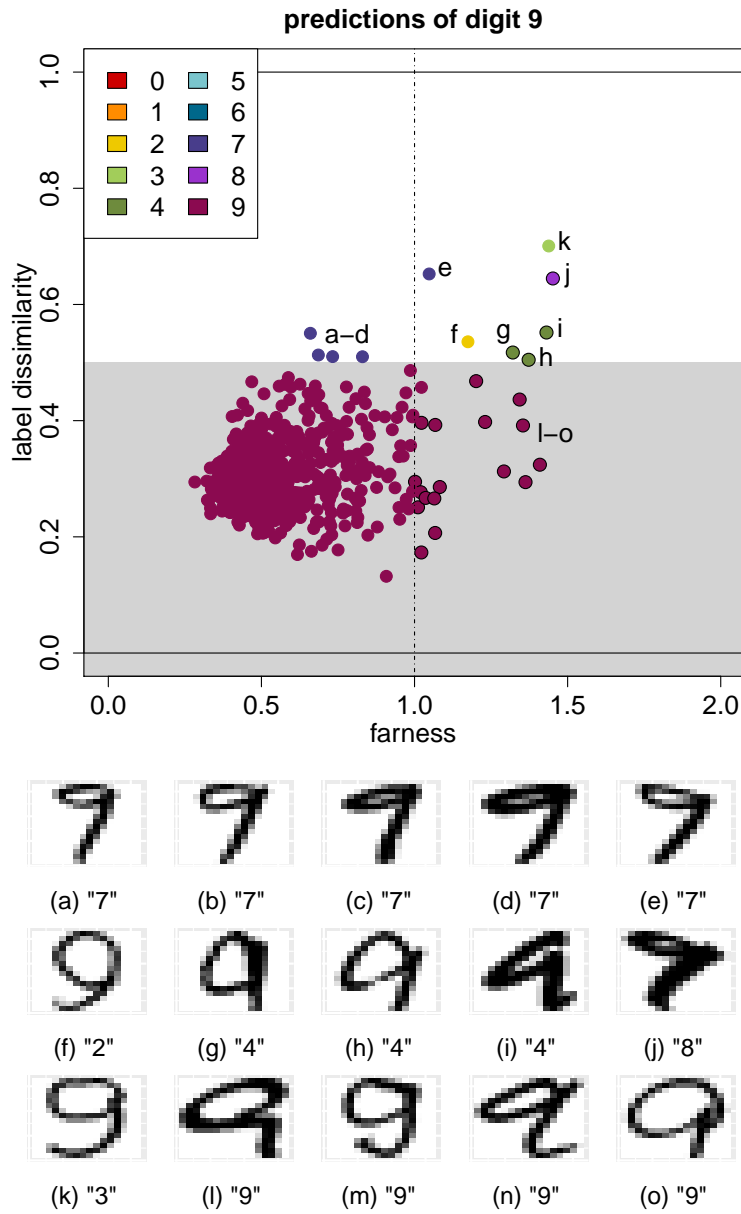


Figure 23: Class map of digit 9, with the images corresponding to the labeled points. Points a-e correspond to images of a 9 with a very flat top part, causing them to be predicted as 7. Other images are predicted as 2, 3, 4, or 8. Images l-o are atypical but predicted correctly.



## A.2 Variables in the spam data

Table 3: The variables in the spam dataset

Variable number(s)	Variable name(s)	Interpretation
1-48	make, address, all, num3d, our, over, remove, internet, order, mail, receive, will, people, report, addresses, free, business, email, you, credit, your, font, 000, money, hp, hpl, george, 650, lab, labs, telnet, 857, data, 415, 85, technology, 1999, parts, pm, direct, cs, meeting, original, project, re, edu, table, conference	percentage of words equal to the given word
49-54	charSemicolon, charRoundbracket, charSquarebracket, charExclamation, charDollar, charHash	fraction of characters equal to ; ( [ ! \$ #
55	capitalAve	average run length of capital letters
56	capitalLong	longest run length of capital letters
57	capitalTotal	total run length of capital letters

### A.3 More on the book review data

Figure 24 shows the class map of the negative reviews in the training data. Also here the farness is relatively concentrated, and in fact part of the horizontal line at around  $LD = 0.25$  is formed by many support vectors (and by symmetry this is also true in Figure 25). Point **a** stands out a bit because it has the highest LD. Indeed review **a** seems to be very positive as can be seen in Table 4. Perhaps this reviewer made a mistake when filling in the stars. Nevertheless, because the classifier was trained on these data review **a** is predicted as negative. Review **b** has the highest farness. It is correctly predicted as negative. The high farness can be explained by the sheer length of this book review. It is over 20,000 characters long, whereas the next longest review in the data is under 10,000 characters and the mean length is under 1000 characters.

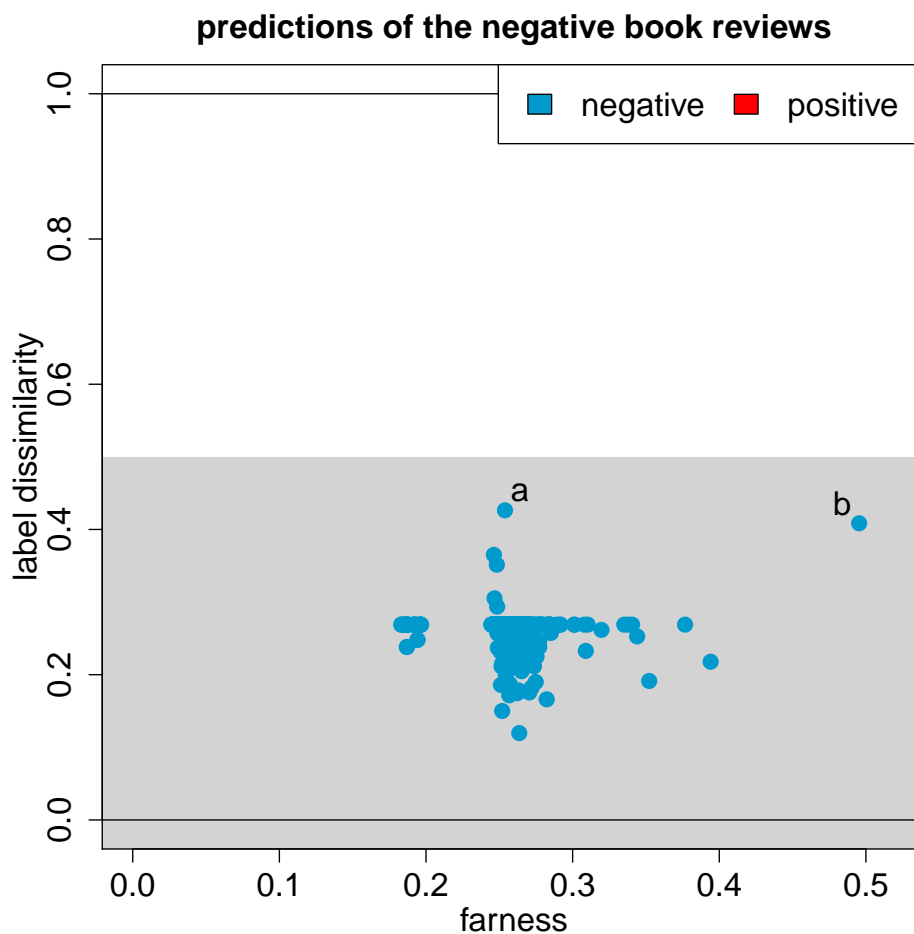


Figure 24: Class map of the negative book reviews in the training data.

Table 4: Excerpts of the negative reviews **a** and **b**.

label	excerpts from the book reviews
<b>a</b>	“the left behind series is the best reading i have ever read.” “when i read the very first book i was hooked” “thank you tim and jerry for such great books”
<b>b</b>	“there is not quite the neglect that nash claimed in these fields” “nash is not the lone voice for these ‘forgotten’ as he claimed”

Figure 25 shows the class map of the positive book reviews in the training data. Two points stand out. Point **c** is nearest to the positive class, and in Table 5 we see that this review is extremely positive. Review **d** has the highest LD indicating its prediction approaches the negative class. It is in fact positive, but there are many negative words due to its rant against other reviews that were negative about the book.

Table 5: Excerpts of the positive reviews **c** and **d**.

label	excerpts from the book reviews
<b>c</b>	“yes, i have seen seventh seal many times, and it is, indeed, stark” “it is imagery that takes your breath away” “it’s just beauty to watch and think about later”
<b>d</b>	“i cannot believe the only 2 bad reviews were given by people who didn’t know the book was written in spanish” “if you want to blame somebody because you cannot read the book, blame the editors for not publishing an english version” “you were careless/stup.. enough to buy a book that you could not read”

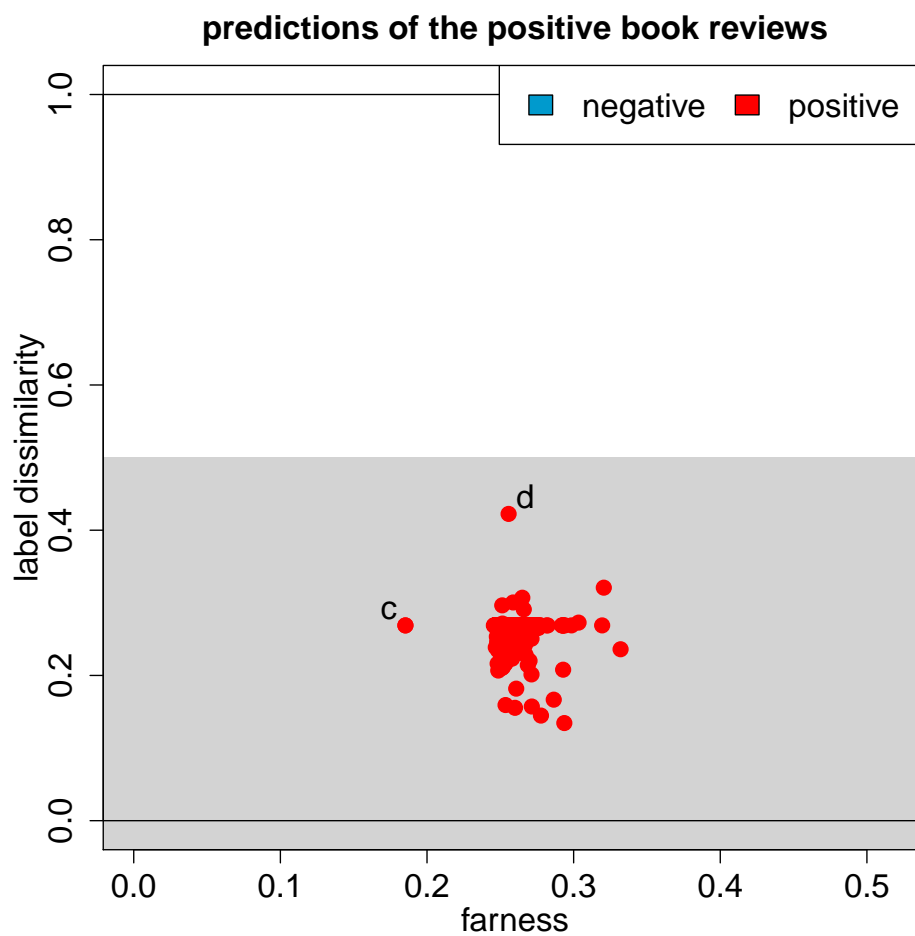


Figure 25: Class map of the positive book reviews in the training data.

## A.4 More on the sweets data

Table 6 provides the names (in German and French) of the products labeled in Figure 13 in the text.

Table 6: Sweets data: names of the labeled objects.

label	Name of the product
a	Brossard Mon pain d'épices au miel (Migros)
b	Kokos Makronli (Migros)
c	X-Cream Sundae Choco Cookies (Burger King)
d	X-Cream Sundae Strawberry (Burger King)
e	Weight Watchers Ice Mokka Becher (Coop)
f	Weight Watchers Ice Schokolade Becher (Coop)
g	Léger Kakao Glace (Migros)
h	Léger Mini Vanille Glace-Stangel (Migros)
i	Erdbeer-Torte, zubereitet (Dr. Oetker)
j	Qualité & Prix Backmischung Rueblitorte (Coop)
k	Erdbeer-Torte (Migros)
l	Leisi Cake Chocolat, Flüssigteig (Nestlé)
m	Nougat Torte (Migros)
n	Dessert Tradition Fondant au Chocolat (Migros)
o	Naturaplan Bio Pulver für Creme á la Vanille (Coop)
p	Milchreis klassisch, Fertigmischung (Migros)
q	Griessbrei Fertigmischung (Migros)
r	Varieta Basis-Creme-Pulver (Migros)
s	Dawa Flan Caramel, Pulver (Wander)
t	Pudding Creme Vanille ohne Zucker, Fertigmischung (Migros)
u	Mousse au Chocolat zartbitter, zubereitet (Dr. Oetker)